Division of Engineering
BROWN UNIVERSITY
PROVIDENCE, RHODE ISLAND 02912

INTERRELATED STRUCTURES OF THE

TRANSPORT SHOCK AND COLLISIONAL RELAXATION

LAYER IN A MULTITEMPERATURE, MULTILEVEL

IONIZED GAS

ANTONIO R. VIÑOLO and JOSEPH H. CLARKE
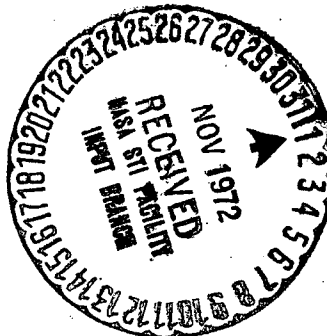
Report No.
GK-31510/1

August 1972

INTERRELATED STRUCTURES OF THE TRANSPORT SHOCK

AND COLLISIONAL RELAXATION LAYER

IN A MULTITEMPERATURE, MULTILEVEL IONIZED GAS

by

Antonio R. Viñolo and Joseph H. Clarke

Division of Engineering
and
Center for Fluid Dynamics
Brown University
Providence, Rhode Island   02912
U.S.A.

August 1972

π

ABSTRACT

The gas dynamic structures of the transport shock and the downstream collisional relaxation layer are evaluated for partially ionized monatomic gases. Elastic and inelastic collisional nonequilibrium effects are taken into consideration. We account in our microscopic model of the atom for three electronic levels. Nonequilibrium processes with respect to population of levels and species plus temperature are considered herein. By using an asymptotic technique the shock morphology is found on a continuum flow basis. The asymptotic procedure gives two distinct layers in which the nonequilibrium effects to be considered are different. A transport shock appears as the inner solution to an outer collisional relaxation layer in which the gas reaches local equilibrium. The results show four main interesting points: (i) on structuring the transport shock, ionization and excitation rates must be included in the formulation, for the asymptotic method does not give frozen flow with respect to the population of the ionized and excited levels, (ii) the sharp rise in electron temperature that might be expected after the transport shock is diffused to its beginning, (iii) the collisional relaxation layer is reduced rationally and accurately to quadrature for special initial conditions which (iv) are obtained from new Rankine-Hugoniot relations for the inner shock. A family of numerical examples is displayed for different flow regimes. Argon and helium models are used in these examples.

I. INTRODUCTION

The possibility of obtaining large gradients by compressing a gas through a shock wave has led many researchers to study transport, transfer and relaxation phenomena both theoretically and experimentally.

It is well known that as the strength of the shock wave becomes larger and larger, radiative and collisional nonequilibrium effects begin to dominate and the thickness of the shock is determined by the characteristic lengths arising from such nonequilibrium processes.

Several authors[1-3] have devoted their attention to the relaxation zone behind a shock wave, taking into account different nonequilibrium phenomena to study the ionization behind it. An excellent review in this field is provided in Ref. 4. Jaffrin[5] studied the transport shock in argon considering the degree of ionization frozen and without including an excited level in the atom model. Chubb[6] included some transport properties and used a bimodal Mott-Smith velocity distribution function to structure the transport shock and the relaxation zone behind it.

Clarke and Ferrari[7] studied the nonequilibrium ionization due to radiation and collision; they found a photoionized precursor in the shock structure. More recently, Clarke and Onorato[8] structured shock waves in monatomic gases using asymptotic arguments. They found different asymptotically embedded layers in which the nonequilibrium effects due to collisional and radiative ionization are uncoupled in each layer. Further applications extending this method are found in works by Pirri and Clarke,[9] and Fainsworth and Clarke.[10]

Finally, Foley and Clarke[11] refined the microscopic gas model of Ref. 8. They found that the shock morphology consisted of certain asymptotically

embedded layers: (i) a nonequilibrium precursor characterized by the absorption of radiation, (ii) a chemically frozen and transparent transport discontinuity, (iii) an optically transparent collisional layer characterized by elastic and inelastic collisions driving the gas to equilibrium, and (iv) a hot radiating tail in local equilibrium.

The purpose of this work is to study the transport shock and the collisional layer in any partially ionized and excited monatomic gas. It will be shown, using an asymptotic argument, that although both layers can be separated asymptotically, they must be evaluated together, for they are intimately interrelated. Furthermore our results will show that the transport shock is not chemically frozen as considered by other authors: Therefore ionization and excitation rates need to be included in the formulation.

Numerical examples are performed for models of argon and helium by using a continuum or Navier-Stokes approach, for different flow regimes. Thermal and chemical nonequilibrium effects are included in the formulation. The results of these calculations justify, a posteriori, the ideas introduced in the present work.

II. MODEL AND STATISTICS

We consider the steady, one dimensional flow of a partially ionized and excited monatomic gas. No applied external electric or magnetic fields are considered herein.

A. Microscopic Model

The monatomic gas atom A is modeled microscopically by three different electronic levels, i.e. a ground level $\underline{1}$ which will provide species $A^{(1)}$, an excited level $\underline{2}$ providing $A^{(2)}$, and the continuum $\underline{c}$ giving the single ionized ion $A^{(+)}$. Therefore, the gas is considered to be a mixture of atoms (both in the ground and excited levels), ions, and electrons. The term heavy particles, denoted by subscript $\underline{h}$, is used when we refer collectively to atoms and ions.

Since the mass of atoms and ions is much greater than that of the electrons, the elastic energy transfer between heavy and light species is considered very difficult and therefore highly inefficient.

We also consider only gases that are difficult to ionize, i.e. the ionization energy is larger than the translational energy throughout the entire flow process. The creation of an ion by inelastic collisions will result in the loss of an amount of energy equal to the ionization energy by the heavy gas or the electron gas depending on which species collides with the atom in the act of ionization. Considering the electron gas, we have two difficult processes which oppose one another: (i) Through elastic collisions the heavy particles and the electrons will try to equilibrate their translational energy, and (ii) every act of ionization by electron impact will substantially reduce the energy of the electrons.

Our gas model also provides for an excited level which is assumed to be very close to the continuum. Therefore excitation also requires a considerable amount of energy but ionization from the excited level is then possible with a much smaller amount of energy.

As the gas enters the shock, the transport mechanisms will convert the initial kinetic energy into thermal energy. However, since the elastic energy transfer between heavy particles and electrons is very inefficient, heavy and light species will have different translational energy. A subsequent collisional relaxation zone will then appear in which all species come to equilibrium.

B. Statistics

Elastic and inelastic collisions are considered in the present work. Mathematical expressions are then needed for the cross sections for the different types of collisions. Although few data are available for excited atoms, the statistics used generally are not the best we could hope for.

There are two types of elastic collisions: (i) elastic collisions between species M and $A^{(2)}$, and (ii) elastic collisions between M and $A^{(1)}$, M denoting any species $A^{(1)}$, $A^{(2)}$, $A^{(+)}$, or electrons. It is known that the effective diameter for the former type of collisions is larger than that for the latter type of collisions. However, since few particles are in the excited level, the excitation energy being almost as large as the ionization energy, the effect of the additional size of the excited atom cross section should not be appreciable in the transport properties.[12,13] Therefore, it will be assumed that the cross sections for elastic collisions between M and $A^{(2)}$ are equal to the cross sections

for collisions between M and $A^{(1)}$.

More specifically, the elastic collisions considered are: collisions between heavy particles, collisions between electrons, and collisions between electrons and heavy species. Since collisions between particles of the same species take place at a much faster rate than collisions between electrons and heavy particles, and the energy transfer between these two species is very inefficient, it is possible to define a heavy particle temperature T_h and an electron temperature T_e in the thermodynamic sense throughout the shock. Therefore, T_h will be, in general, different from T_e .

For the inelastic collisions, we only consider transitions by electron impact. This is due to the fact that, since the gas is already sufficiently ionized ahead of the shock, the most efficient mechanisms for further excitation or ionization are those by electron-atom inelastic collisions.[14] It has been shown previously that the transport shock and the collisional relaxation layer are transparent to any radiation.[11] Therefore any radiative effects need not be included in the present work. Thus, the following parallel chemical reactions will account for the inelastic transitions:

$$\left.\begin{array}{ll} A^{(1)} + e \rightleftharpoons A^{(+)} + e + e & \text{(1-c transitions)} , \\ A^{(1)} + e \rightleftharpoons A^{(2)} + e & \text{(1-2 transitions)} , \\ A^{(2)} + e \rightleftharpoons A^{(+)} + e + e & \text{(2-c transitions)} . \end{array}\right\} \qquad (2.1)$$
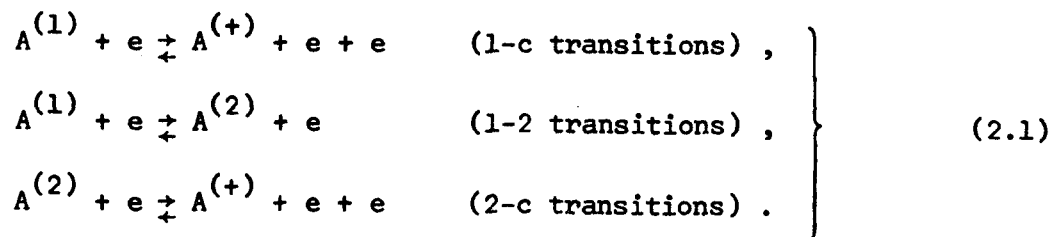
As a result of the aforementioned nonequilibrium rate processes, the gas is not generally in local equilibrium with respect to population of levels and species $\underline{or}$ temperature.

To make the problem more tractable mathematically, we now introduce

several a priori assumptions which will be justified a posteriori:

(a) Small ion-slip: The ion-atom elastic collision cross section due to the charge exchange mechanism is very large, so that the ion-atom mean free path is small compared to the shock thickness. There will then be many collisions between atoms and ions and therefore their temperature and velocities will be equal.[5]

(b) Quasi-charge neutrality: Charge separation effects have been neglected because the Debye length is much smaller than any other characteristic length.[5] Also the induced electric field is negligible.[5] Thus, we assume that the ion and electron number densities are equal and therefore all the species have the same macroscopic velocity.

(c) Initially frozen elastic and inelastic collisions: It is possible for the upstream flow ahead of the shock to be locally out of equilibrium with respect to population of levels and species and/or temperature. In that situation a precursor will appear. This nonequilibrium precursor can be structured, for instance, by the absorption of radiation coming from a hot layer behind the shock. Since the characteristic length of this precursor is much larger than any characteristic length of interest to us,[11] the upstream flow is seen as frozen on the length scale of the shock. Even in the case when T_h and T_e are different ahead of the shock, $(T_h - T_e)$ is small compared to its value behind the transport shock. Since the elastic collision energy transfer is proportional to that difference, we can create an artificial state of equilibrium upstream of the shock without introducing an appreciable error. This is done by subtracting from the elastic collision energy transfer term, denoted by E , its numerical value at the front of the shock $E(a)$. The inelastic collisions can be treated in the same way, since the electron

temperature upstream is sufficiently low to neglect the ionization and excitation by electron impact ahead of the shock. This assumption will be clarified later on.

III. FORMULATION

Under the assumptions and the model as described in Section II, the equations governing our problem are then the equations of state, continuity, momentum, energy, electron energy, ionization and excitation rates. Let n_1 , n_2 , n_e denote the number densities of atoms in the ground level, atoms in the excited level, and electrons (or ions) respectively, u the velocity, p the pressure, ρ the mass density of the mixture, α the degree of ionization, β the degree of excitation, T_j the ionization temperature, T_ℓ the excitation temperature, R the gas constant per unit mass of atoms, and m_h the mass of an atom (or ion). Then we have

$$\rho = m_h(n_1 + n_2 + n_e) \ , \qquad \alpha \equiv \frac{n_e}{n_1 + n_2 + n_e} \ , \qquad \beta \equiv \frac{n_2}{n_1 + n_2 + n_e} \ . \tag{3.1}$$

The enthalpy per unit mass of the mixture, H , shall be written as

$$H = R \left[\frac{5}{2}(T_h + \alpha T_e) + \alpha T_j + \beta T_\ell \right]. \tag{3.2}$$

Then our equations are

$$p = \rho R(T_h + \alpha T_e) \ , \tag{3.3}$$

$$\rho u = G \ , \tag{3.4}$$

$$p + \rho u^2 - \frac{4}{3} \mu \frac{du}{dx} = GV \ , \tag{3.5}$$

$$G \left[\frac{u^2}{2} + \frac{5}{2}R(T_h + \alpha T_e) + \alpha R T_j + \beta R T_\ell \right] - \frac{4}{3} \mu u \frac{du}{dx} - K_h \frac{dT_h}{dx} - K_e \frac{dT_e}{dx} = G \frac{W^2}{2} \ ,$$

$$\tag{3.6}$$

wherein (3.5) and (3.6) μ , K_h , K_e are the coefficients of shear viscosity of the mixture, thermal conductivity of the heavy particles, and thermal conductivity of the electrons respectively. The electron energy equation can be written as[11]

$$\frac{3}{2}\frac{dT_e}{dx} + \frac{T_e}{u}\frac{du}{dx} - \frac{1}{GR\alpha}\frac{d}{dx}\left(K_e\frac{dT_e}{dx}\right) = E - \frac{T_j}{\alpha}\frac{d\alpha}{dx} - \frac{T_\ell}{\alpha}\frac{d\beta}{dx} , \qquad (3.7)$$

E being the energy transfer term between heavy particles and electrons by elastic collisions, and the other two relevant terms on the right denote the energy transfer between the same two species by inelastic collisions, leading to essential new effects.

Let $\left(\kappa_{mn}\right)_{i-j}$ denote the reaction rate coefficients in the chemical reaction between particles of the mth and nth species for transition from the ith to the jth level. Since as discussed in Section II, the only reactions considered are those by electron impact, we let

$$\left(\kappa_{mn}\right)_{i-j} \equiv \left(\kappa_{eh}\right)_{i-j} = \kappa_{i-j} . \qquad (3.8)$$

Then from (2.1) and (3.1), the population rate equations are

$$\frac{d\alpha}{dx} = G^{-1}m_h\left[\kappa_{1-c}\left(\frac{\rho}{m_h}\right)^2\alpha(1-\alpha-\beta) - \kappa_{c-1}\left(\frac{\rho}{m_h}\right)^3\alpha^3 + \kappa_{2-c}\left(\frac{\rho}{m_h}\right)^2\alpha\beta - \kappa_{c-2}\left(\frac{\rho}{m_h}\right)^3\alpha^3\right] ,$$

$$\qquad (3.9)$$

$$\frac{d\beta}{dx} = G^{-1}m_h\left[\kappa_{1-2}\left(\frac{\rho}{m_h}\right)^2\alpha(1-\alpha-\beta) - \kappa_{2-1}\left(\frac{\rho}{m_h}\right)^2\alpha\beta + \kappa_{c-2}\left(\frac{\rho}{m_h}\right)^3\alpha^3 - \kappa_{2-c}\left(\frac{\rho}{m_h}\right)^2\alpha\beta\right] .$$

$$\qquad (3.10)$$

If inelastic collisions by heavy-heavy encounters were important in

C

the ionization and excitation processes, more terms would be required on the right hand side of the rate equations. According to our assumptions, transitions by heavy particle impact are negligible and therefore are not included in the formulation.

It is expeditious to utilize the fact that the reverse reaction rate coefficients κ_{j-i} can be expressed as functions of the different forward reaction rate coefficients κ_{i-j} through equilibrium considerations. Then, from (3.9) and (3.10) we obtain

$$\kappa_{c-1}(T_e) = \kappa_{1-c}(T_e) \frac{m_h}{\rho} \frac{1-\alpha_E-\beta_E}{\alpha_E^2} \;, \quad \kappa_{c-2}(T_e) = \kappa_{2-c}(T_e) \frac{m_h}{\rho} \frac{\beta_E}{\alpha_E^2} \;, \qquad (3.11)$$

$$\kappa_{2-1}(T_e) = \kappa_{1-2}(T_e) \frac{1-\alpha_E-\beta_E}{\beta_E} \;, \qquad (3.12)$$

where the subscript $\underline{E}$ denotes reference equilibrium conditions at ρ and T_e. The remaining κ's can conveniently be written as lengths for gas dynamic purposes.[7] A local characteristic length for the ionization process is seen to be[14]

$$\lambda_\alpha \equiv \frac{m_h u}{\kappa_{1-c}\rho(1-\alpha-\beta)} \;. \qquad (3.13)$$

Similarly, from Ref. 5, we have expressions for the different transport coefficients and the elastic collision energy transfer term E expressed in terms of lengths

$$\mu = \rho(RT_h)^{1/2}\lambda_\mu \;, \qquad (3.14)$$

$$K_h = \rho R(RT_h)^{1/2}\lambda_{Kh} \;, \qquad (3.15)$$

$$K_e = \alpha\rho R(RT_e)^{1/2}\lambda_{ke} \;, \qquad (3.16)$$

$$E = (RT_e)^{1/2} \frac{T_h - T_e}{u} \frac{1}{\lambda_e} \quad , \tag{3.17}$$

where λ_μ, λ_{Kh}, λ_{Ke}, and λ_e are lengths characterizing the different transport and transfer phenomena. In the Appendix expressions are provided for the different forward reaction rate coefficients and for the characteristic lengths defined above as functions of the dependent variables. Thus we have seven equations in the unknowns u, ρ, p, T_h, T_e, α, and β.

The equations will now be written in dimensionless form. We define a dimensionless independent variable η through the relation

$$d\eta = \lambda_\alpha^{-1} dx \quad , \quad \eta = \int_o^x \lambda_\alpha^{-1}(x)dx \quad . \tag{3.18}$$

Let $(T_e)_b$ be the electron temperature at station $\underline{b}$ inside the shock. The significance of station $\underline{b}$ will become clear later on. Then the following dimensionless dependent variables are found natural and appropriate to the problem

$$\hat{T}_i = \frac{T_i}{(T_e)_b} \quad , \quad \hat{u} = \frac{u}{[R(T_e)_b]^{1/2}} \quad , \quad \hat{\rho} = \rho \frac{[R(T_e)_b]^{1/2}}{G} \quad , \quad \hat{p} = \frac{p}{G[R(T_e)_b]^{1/2}} \quad , \tag{3.19}$$

where T_i stands for T_h, T_e, T_j, or T_ℓ accordingly.

We substitute the relevant lengths for the transport coefficients and the elastic collision energy transfer term into the equations and make them dimensionless following (3.18), (3.19). We have

$$\hat{p} = \hat{\rho}(\hat{T}_h + \alpha \hat{T}_e) \quad , \tag{3.20}$$

$$\hat{\rho}\hat{u} = 1 \quad , \tag{3.21}$$

$$\hat{p} + \hat{u} - \frac{4}{3}\frac{\lambda_\mu}{\lambda_\alpha}\hat{\rho}\hat{T}_h^{1/2}\frac{d\hat{u}}{d\eta} = \frac{V}{[R(T_e)_b]^{1/2}} , \qquad (3.22)$$

$$\frac{5}{2}(\hat{T}_h + \alpha\hat{T}_e) + \alpha\hat{T}_j + \beta\hat{T}_\ell + \frac{\hat{u}^2}{2} - \frac{4}{3}\frac{\lambda_\mu}{\lambda_\alpha}\hat{T}_h^{1/2}\frac{d\hat{u}}{d\eta} - \frac{\lambda_{Kh}}{\lambda_\alpha}\hat{\rho}\hat{T}_h^{1/2}\frac{d\hat{T}_h}{d\eta}$$

$$- \frac{\lambda_{Ke}}{\lambda_\alpha}\alpha\hat{\rho}\hat{T}_e^{1/2}\frac{d\hat{T}_e}{d\eta} = \frac{W^2}{2R(T_e)_b} , $$

$$(3.23)$$

$$\frac{1}{\hat{T}_j}\left[\frac{3}{2}\frac{d\hat{T}_e}{d\eta} + \frac{\hat{T}_e}{\hat{u}}\frac{d\hat{u}}{d\eta} - \frac{1}{\alpha}\frac{d}{d\eta}\left(\frac{\lambda_{Ke}}{\lambda_\alpha}\alpha\hat{\rho}\hat{T}_e^{1/2}\frac{d\hat{T}_e}{d\eta}\right)\right] = \frac{1}{\hat{T}_j}\frac{\lambda_\alpha}{\lambda_e}\frac{\hat{T}_e^{1/2}}{\hat{u}}(\hat{T}_h - \hat{T}_e)$$

$$- \frac{1}{\alpha}\frac{d\alpha}{d\eta} - \frac{1}{\alpha}\frac{\hat{T}_\ell}{\hat{T}_j}\frac{d\beta}{d\eta} , \quad (3.24)$$

$$\frac{1}{\alpha}\frac{d\alpha}{d\eta} = \left[1 - \frac{\alpha^2}{1-\alpha-\beta}\frac{1-\alpha_E-\beta_E}{\alpha_E^2}\right] + \frac{\kappa_{2-c}}{\kappa_{1-c}}\frac{\frac{\beta}{\alpha}}{\frac{1-\alpha-\beta}{\alpha}}\left[1 - \frac{\alpha^2}{\beta}\frac{\beta_E}{\alpha_E^2}\right] \equiv \hat{I}_1 , \qquad (3.25)$$

$$\frac{1}{\alpha}\frac{d\beta}{d\eta} = \frac{\kappa_{1-2}}{\kappa_{1-c}}\left[1 - \frac{\beta}{1-\alpha-\beta}\frac{1-\alpha_E-\beta_E}{\beta_E}\right] - \frac{\kappa_{2-c}}{\kappa_{1-c}}\frac{\frac{\beta}{\alpha}}{\frac{1-\alpha-\beta}{\alpha}}\left[1 - \frac{\alpha^2}{\beta}\frac{\beta_E}{\alpha_E^2}\right] \equiv \hat{I}_2 . \quad (3.26)$$

From the above equations, we see that we have four ratios of character-istic lengths and two ratios of forward rate coefficients which could be

converted in length ratios very easily, but we do not wish to do so here.

Now, from the definition of λ_e and λ_{Ke} , we can see that both

lengths are comparable and of the same order of magnitude. It is also

clear from the expressions of λ_μ and λ_{Kh} that both are of the same

order of magnitude. Moreover, numerical considerations tell us that λ_{Ke}

and λ_{Kh} can be comparable and that λ_α is the largest of all the lengths

introduced herein. Usually, the above lengths satisfy the following

inequalities:

$$\lambda_\mu \simeq \lambda_{Kh} < \lambda_{Ke} \simeq \lambda_e \ll \lambda_\alpha . \tag{3.27}$$

Notice that since the excited and the continuum levels are considered

to be very close together, λ_α also characterizes the excitation process.

From the above ordering of the characteristic lengths we see that if

the problem or phenomena of interest to us occurs in a length of order

λ_α , we can neglect all the transport effects in (3.20)-(3.26).

IV. ASYMPTOTICS

Let us now construct a mathematical representation of our physical model discussed in Section II-A. The gas can be represented by constructing three limits. If m_e is the electron mass, let

$$\delta \equiv (m_h/m_e)^{1/2} \to \infty \; , \quad \hat{T}_j \to \infty \; , \quad \left(1 - \frac{\hat{T}_\ell}{\hat{T}_j}\right) \to 0^+ \; , \qquad (4.1a,b,c)$$

such that

$$\hat{T}_j \left[1 - \frac{\hat{T}_\ell}{\hat{T}_j}\right] = O(1) \; , \quad \Gamma_1 \equiv \frac{1}{\hat{T}_j} \frac{\lambda_\alpha}{\lambda_e} = O(1) \; , \quad \Gamma_2 \equiv \frac{\kappa_{2-c}}{\kappa_{1-c}} \frac{\frac{\beta}{\alpha}}{\frac{1-\alpha-\beta}{\alpha}} = O(1) \; ,$$

$$(4.2a,b,c)$$

the reasons behind (4.2) will appear clear as we proceed.

Notice that only one of the three limits (4.1) introduced is independent. The last two are related through (4.2a), and δ and $\hat{T}_j$ are connected in Γ_1. In Γ_2 an additional relation is provided between two of the three reaction rate coefficients.

From the physics of Section II, and from (4.1c) it follows that

$$\frac{\beta}{\alpha} \to 0 \; , \qquad (4.3)$$

which means that the excited level is highly depopulated, i.e. because the excited and the continuum levels are very close together, it is easier to ionize from the excited level, rather than from the ground level, resulting in its consequent depletion. Similarly, from our physical model and (4.1c) it follows that

$$\frac{\kappa_{1-2}}{\kappa_{1-c}} = O(1) \quad , \quad \frac{\kappa_{2-c}}{\kappa_{1-c}} \to \infty \quad . \qquad (4.4a,b)$$

From our expressions for the forward reaction rate coefficients (Appendix B) and our limit construct (4.1) together with (4.2a) we can verify the validity of (4.4). Notice that (4.3) and (4.4b) are not independent for they are related by (4.2c).

At this point, under our limit, other dimensionless dependent variables, e.g. $\hat{T}_h$, $\hat{T}_e$, $\hat{u}$, $\hat{\rho}$, and $\hat{p}$ are considered $O(1)$. We are now in a position to study our equations and to try to simplify them by using the above orders of magnitude under the limits constructed.

A. Outer Solution

First consider the collisional relaxation process. The characteristic length scaling such phenomena is seen to be λ_α defined in (3.13). We assume that derivatives with respect to $\eta \sim x/\lambda_\alpha$ are $O(1)$ under our limit. From the discussion of the different characteristic lengths introduced in Section III and from (4.2b), we see that λ_α is much larger than any of the other characteristic lengths. Therefore, on studying the collisional relaxation, it is permissible to neglect all the transport effects in (3.20)-(3.26). Thus, the layer in which the transport mechanisms are important, referred to as the transport shock, is seen to have zero thickness on the length scale defined by λ_α. The characteristic electron temperature $(T_e)_b$ introduced in Section III appears now as the electron temperature just behind the transport shock. Therefore in the outer solution or collisional relaxation layer, the momentum and energy equations (3.22) and (3.23)

become algebraic! It is possible then to evaluate the integration constants in the right members of (3.22), (3.23) anywhere inside the collisional layer. Evaluating them just behind the transport shock at stage <u>b</u>, (3.23) becomes

$$\frac{5}{2}\left(\hat{T}_h + \alpha\hat{T}_e - (\hat{T}_h)_b - \alpha_b\right) + \hat{T}_j(\alpha-\alpha_b)\left[1 + \frac{\hat{T}_\ell}{\hat{T}_j}\frac{\beta-\beta_b}{\alpha-\alpha_b}\right] + \frac{\hat{u}^2-\hat{u}_b^2}{2} = 0 \qquad (4.5)$$

From (4.1c) and (4.3) we can neglect the second term in brackets in (4.5) as compared to one. Since the first and last terms are $O(1)$, it is necessary that

$$T_j(\alpha-\alpha_b) = O(1) \ , \quad \text{or} \quad \alpha-\alpha_b = O\left(\frac{1}{\hat{T}_j}\right). \qquad (4.6)$$

Our limit (4.1b) strictly implies that α does not change, from its value behind the transport shock, over the collisional layer. However, it is known[7,8] that, for appreciable ionization, the electron temperature does not have to be close to $\hat{T}_j$. For all the numerical examples considered, $\hat{T}_j$ tends very weakly to its limits $(\hat{T}_j \sim 10)$, and therefore considerable ionization can occur. Moreover, by neglecting $(1/\hat{T}_j)$ compared to unity, the ionization can be predicted very accurately with a 16-20% error.[7,8]

We now turn to the population rate equations. The brackets in (3.25), (3.26) account for the combined forward and reverse reactions. Their numerical values vary between zero and one. Only when the flow reaches equilibrium, will the forward and reverse reactions balance and give zero for the bracket terms.

In (3.25). both the right and left members are $O(1)$ under our limit. Then, the population rate equation for the ionized level remains differential

over the outer solution.

In (3.26), the left member is $O(\beta/\alpha)$ which is small under (4.3). The right hand side is $O(1)$ under (4.2c) and (4.4a). Thus, the left member of (3.26) is negligible and β is given locally in terms of the other dependent variables by equating to zero the right-hand side of (3.26). The population rate equation for the excited level reduces to algebraic!

If in (3.24) we replace (See Appendix) $\dfrac{d\alpha}{d\eta}$ and $\dfrac{d\beta}{d\eta}$ by their respective expressions $\hat{I}_1$ and $\hat{I}_2$, we see that the right member is $O(1)$ while the left-hand side is $O\left(\dfrac{1}{T_j}\right)$ and therefore it can be neglected under (4.1b). The electron energy equation also reduces to algebraic over the outer solution. Namely, it reads

$$\hat{E} - (\hat{I}_1 + \hat{I}_2) = 0 , \tag{4.7}$$

which means, physically, that the heating (cooling) of the electron gas through elastic collisions with the heavy particles is balanced by the cooling (heating) due to inelastic collisions between the same two species.

We have shown that, over the outer solution, the system of five differential equations (3.20) - (3.26) reduces to only one differential equation, the one governing the population of the ionized level. Then, all the dependent variables, except the degree of ionization, will adjust to local conditions and can be expressed as functions of α , the only non-equilibrium variable, since α_E and β_E can be expressed in terms of $\hat{T}_e$ and $\hat{\rho}$. We say that, over the collisional layer, the flow is in a state of "autolocal equilibrium." The outer solution is then very simple to obtain, for the problem is reduced rationally to quadrature.

B. Inner Solution

By reducing our system of equations over the outer solution to only one differential equation, it is clear that the boundary conditions at the front of the shock wave, station $\underline{a}$, cannot be satisfied. On the scale λ_α, this means that a geometrically thin boundary layer must exist in which at least some of the derivatives in (3.22)-(3.24) and (3.26) tend to infinity. Considering the two lengths appearing in (4.2b), x must be scaled by λ_e instead of λ_α according to

$$d\zeta \equiv \lambda_e^{-1} dx \ , \quad \text{or} \quad \zeta = \int_o^x \lambda_e^{-1} dx \ . \tag{4.8}$$

Then over the boundary layer we obtain

$$\hat{p} = \hat{\rho}(\hat{T}_h + \alpha \hat{T}_e) \ , \tag{4.9}$$

$$\hat{\rho}\hat{u} = 1 \ , \tag{4.10}$$

$$\hat{p} + \hat{u} - \frac{4}{3} \frac{\lambda_\mu}{\lambda_e} \hat{\rho}\hat{T}_h^{1/2} \frac{d\hat{u}}{d\zeta} = \frac{V}{[R(\hat{T}_e)_b]^{1/2}} \ , \tag{4.11}$$

$$\frac{5}{2}(\hat{T}_h + \alpha \hat{T}_e) + \alpha \hat{T}_j + \beta \hat{T}_\ell + \frac{\hat{u}^2}{2} - \frac{4}{3} \frac{\lambda_\mu}{\lambda_e} \hat{T}_h^{1/2} \frac{d\hat{u}}{d\zeta} - \frac{\lambda_{Kh}}{\lambda_e} \hat{\rho}\hat{T}_h^{1/2} \frac{d\hat{T}_h}{d\zeta}$$

$$-\alpha \frac{\lambda_{Ke}}{\lambda_e} \hat{\rho}\hat{T}_e^{1/2} \frac{d\hat{T}_e}{d\zeta} = \frac{W^2}{2R(T_e)_b} \ , \tag{4.12}$$

$$\frac{3}{2}\frac{d\hat{T}_e}{d\zeta} + \frac{\hat{T}_e}{\hat{u}}\frac{d\hat{u}}{d\zeta} - \frac{1}{\alpha}\frac{d}{d\zeta}\left[\frac{\lambda_{Ke}}{\lambda_e}\alpha\rho\hat{T}_e^{1/2}\frac{d\hat{T}_e}{d\zeta}\right] = \frac{\hat{T}_e^{1/2}}{\hat{u}}(\hat{T}_h - \hat{T}_e)$$

$$- \frac{1}{\alpha}\left[\hat{T}_j\frac{d\alpha}{d\zeta} + \hat{T}_\ell\frac{d\beta}{d\zeta}\right], \qquad (4.13)$$

$$\frac{1}{\alpha}\frac{d\alpha}{d\zeta} = \frac{1}{\hat{T}_j}\frac{1}{\Gamma_1}\left\{\left[1 - \frac{\alpha^2}{1-\alpha-\beta}\frac{1-\alpha_E-\beta_E}{\alpha_E^2}\right] + \Gamma_2\left[1 - \frac{\alpha^2}{\beta}\frac{\beta_E}{\alpha_E^2}\right]\right\}, \qquad (4.14)$$

$$\frac{1}{\alpha}\frac{d\beta}{d\zeta} = \frac{1}{\hat{T}_j}\frac{1}{\Gamma_1}\left\{\frac{\kappa_{1-2}}{\kappa_{1-c}}\left[1 - \frac{\beta}{1-\alpha-\beta}\frac{1-\alpha_E-\beta_E}{\beta_E}\right] - \Gamma_2\left[1 - \frac{\alpha^2}{\beta}\frac{\beta_E}{\alpha_E^2}\right]\right\}. \qquad (4.15)$$

It is clear that in a layer scaled by $\lambda_e \ll \lambda_\alpha$, no appreciable

ionization or excitation can occur, since λ_α characterizes both the

ionization and excitation processes. Effectively (4.14) states that

$\frac{1}{\alpha}\frac{d\alpha}{d\zeta}$ is $0\left(\frac{1}{\hat{T}_j}\right)$ which is small under (4.1b); however $\frac{\hat{T}_j}{\alpha}\frac{d\alpha}{d\zeta}$ is $0(1)$.

The right-hand side of (4.15) is $0\left(\frac{1}{\hat{T}_j}\right)$ while its left member is higher or-

der because everywhere β is much smaller than α. Therefore in (4.13) we

could neglect $\frac{1}{\alpha}\frac{d\beta}{d\zeta}$ as compared to $\frac{1}{\alpha}\frac{d\alpha}{d\zeta}$. For the reasons explained in

the Appendix we prefer to substitute these derivatives by their corresponding

expressions in the right of (4.14) and (4.15). Since λ_{Ke} and λ_e are

comparable lengths, the left member of (4.13) is $0(1)$. Therefore, although

ionization and excitation rates are small, these rates must be included in
(4.13). From the numerical point of view, it is possible to consider α
and β as constant at their initial value over the inner solution; therefore,
we do not wish to carry the asymptotic argument any further.

Notice that, since λ_e can be comparable to λ_{Ke}, λ_{Kh} and λ_μ the
transport terms must be included in the momentum and energy equations. In
(4.12), $\alpha\hat{T}_j$ and $\beta\hat{T}_\ell$ will cancel with similar terms appearing in the
integration constant W.

Then over the inner solution, (i) the transport effects are relevant,
and (ii) although ionization and excitation are small, the inner solution
does not give frozen flow with respect to the population of ionized and
excited levels, for excitation and ionization rates must be included in the
electron energy equation. We shall take α and β constant at their
initial value. We say that inside the transport shock the flow is in a
state of "slight ionization and excitation."

Finally, we must mention that the error factor introduced by the
asymptotic procedure is seen to be $\left[1 + 0\left(\frac{1}{T_j}\right)\right]$ over both the outer and
inner solutions.

V. JUMP CONDITIONS

It is possible for the upstream flow not to be in local equilibrium. In that case a precursor will appear ahead of the shock front (see Section II). However, the flow in this precursor is seen as frozen in the length scales defined by either λ_e or λ_α . There is also a possibility, depending on the flow conditions, for the existence of a hot radiating tail in equilibrium, behind the collisional layer, in which the flow will reach complete thermodynamic equilibrium.[11] Even in that situation, since this tail is structured by the absorption of radiation, the flow in this tail is seen to be in complete equilibrium on the length scale defined by λ_α . It is possible then, from our equations to evaluate the jump conditions, denoted by [ ] , across both the outer and inner solutions.

A. Outer Shock Jump Conditions

At the end of the collisional layer (station $\underline{c}$), thermal equilibrium between the species is reached, so that $T_{hc} = T_{ec} = T_c$. Then, from our equations (3.20) - (3.26) we can get the outer jump conditions, because the flow derivatives outside the shock vanish in the length scale of the outer solution. Therefore we get, in the physical variables

$$\left[\rho u\right]_c^a = 0 \ , \quad \left[p + \rho u^2\right]_c^a = 0 \ , \quad \left[H + \frac{u^2}{2}\right]_c^a = 0 \ , \tag{5.1}$$

together with the equation of state and

$$(T_h)_c = (T_e)_c = T_c \ , \quad \alpha_c = \alpha_E(T_c, \rho_c) \ , \quad \beta_c = \beta_E(T_c, \rho_c) \ . \tag{5.2}$$

Therefore, the flow at the end of the collisional layer will be in local

equilibrium.

B. Jump Conditions Across Inner Shock

Since $\lambda_e \ll \lambda_\alpha$, the flow derivatives in the collisional layer measured in the length scale λ_e will be vanishing small. The same statement holds if there is a precursor ahead of the shock. Then, if we know the flow conditions ahead of the shock (station a) we can evaluate the flow conditions just behind the transport shock (station b) from (4.9) - (4.15). These jump conditions are given, in the physical variables, by

$$\left[\rho u\right]_b^a = 0 \; , \quad \left[p + \rho u^2\right]_b^a = 0 \; , \quad \left[H + \frac{u^2}{2}\right]_b^a = 0 \; . \tag{5.3}$$

together with $\alpha = \alpha_a = \alpha_b$, $\beta = \beta_a = \beta_b$, the equation of state and

$$E(b) = [\lambda_\alpha(b)]^{-1}[T_j \hat{I}_1(b) + T_\ell \hat{I}_2(b)] \; , \tag{5.4}$$

from the electron equation (4.13).

Note that (5.4) does not give the generally accepted $\left[T_e\right]_b^a = 0$ across the transport shock, but tells that there is an energy balance between the electron-heavy particles elastic and inelastic collisions.

Although the conditions of shock discussed here do not appear to be classical Rankine-Hugoniot relations, they effectively are. For the type of shocks considered and under the assumptions made, (5.4) plays the role of a thermodynamic equation of state.

VI. METHOD OF SOLUTION

From our previous discussion, the method for structuring the shock appears clear: (a) Evaluate the jump conditions across the inner and outer shocks as discussed in Section V. (b) Solve the collisional layer: the forward reaction rate coefficients can be expressed as functions of $\hat{T}_e$ [16,17] and α_E and β_E are also functions of $\hat{\rho}$ and $\hat{T}_e$. Then from (3.20) – (3.24) and (3.26), which reduce to algebraic form over the outer solution, we can express $\hat{\rho}, \hat{u}, \hat{p}, \hat{T}_h, \hat{T}_e$ and β as functions of α alone. Substituting these functions in (3.25), we have an equation of the form

$$\frac{d\alpha}{f(\alpha)} = d\eta . \tag{6.1}$$

Eq. (6.1) is integrated numerically, by Simpson's rule, between the limits $\alpha = \alpha_a = \alpha_b$ and $\alpha = \alpha_c$ which are known from the jump conditions. This integration will give $\alpha = \alpha(\eta) = \alpha(x)$. Once $\alpha(x)$ is known, we can compute the spatial distribution of the remaining dependent variables since they are given in terms of α. The solution over the collisional layer is very simple to obtain because the problem is reduced to quadrature. (c) Solve the inner solution: The constants of integration are evaluated at a . Considering α and β constant over the transport shock, we introduce an auxiliary dependent variable z through

$$\frac{d\hat{T}_e}{d\zeta} = \frac{\lambda_e}{\lambda_{Ke}} \frac{\hat{u}}{\hat{T}_e^{1/2}} z . \tag{6.2}$$

Using the equations of state and continuity to eliminate pressure and density, we solve for the different derivative terms. We then eliminate

the independent variable ζ , by dividing all the equation by (6.2) to get

$$\frac{d\hat{u}}{d\hat{T}_e} = \frac{\dfrac{\hat{T}_h + \alpha\hat{T}_e}{\hat{u}} - \dfrac{(\hat{T}_h)_a + \alpha(\hat{T}_e)_a}{\hat{u}_a} + \hat{u} - \hat{u}_a}{\dfrac{4}{3}\dfrac{\lambda_\mu}{\lambda_{Ke}}\left(\dfrac{\hat{T}_h}{\hat{T}_e}\right)^{1/2} z} \quad , \tag{6.3}$$

$$\frac{d\hat{T}_h}{d\hat{T}_e} = \frac{\dfrac{3}{2}(\hat{T}_h + \alpha\hat{T}_e) + \left(\dfrac{\hat{u}}{\hat{u}_a} - \dfrac{5}{2}\right)\left[(\hat{T}_h)_a + \alpha(\hat{T}_e)_a\right] - \dfrac{1}{2}(\hat{u} - \hat{u}_a)^2 - \alpha z}{\dfrac{\lambda_{Kh}}{\lambda_{Ke}}\left(\dfrac{\hat{T}_h}{\hat{T}_e}\right)^{1/2} z} \quad , \tag{6.4}$$

$$\frac{dz}{d\hat{T}_e} = \left\{ \frac{3}{2}\frac{\lambda_e}{\lambda_{Ke}}\frac{\hat{u}}{\hat{T}_e^{1/2}} z + \frac{\hat{T}_e}{\hat{u}}\frac{d\hat{u}}{d\zeta} - \left[\frac{\hat{T}_e^{1/2}}{\hat{u}}(\hat{T}_h - \hat{T}_e) - Y_a\right] + \frac{\hat{T}_j}{\alpha}\left[\frac{d\alpha}{d\zeta} - \left(\frac{d\alpha}{d\zeta}\right)_a\right] \right.$$

$$\left. + \frac{\hat{T}_\ell}{\alpha}\left[\frac{d\beta}{d\zeta} - \left(\frac{d\beta}{d\zeta}\right)_a\right] \right\} \times \left[\frac{\lambda_e}{\lambda_{Ke}}\frac{\hat{u}}{\hat{T}_e^{1/2}} z\right]^{-1} \quad , \tag{6.5}$$

wherein

$$Y_a = \frac{\lambda_e}{(\lambda_e)_a}\frac{(\hat{T}_e)_a^{1/2}}{\hat{u}_a}\left[(\hat{T}_h)_a - (\hat{T}_e)_a\right] \quad , \tag{6.6}$$

and in (6.5) $\dfrac{d\hat{u}}{d\zeta}$, $\dfrac{d\alpha}{d\zeta}$, $\dfrac{d\beta}{d\zeta}$ should be replaced by their appropriate expressions (6.3), (4.14) and (4.15) in terms of the other variables.

Numerical integration of (6.3) - (6.5) is initiated at the four-dimensional singular point at state $\underline{b}$ using the limiting values of the derivatives $\dfrac{d\hat{u}}{d\hat{T}_e}$, $\dfrac{d\hat{T}_h}{d\hat{T}_e}$, $\dfrac{d\hat{z}}{d\hat{T}_e}$ as determined from (6.3) - (6.5) by l'Hôpital's rule.

The numerical integration scheme used is a modification of the method described in Ref. 18. Eqs. (6.3) - (6.5), in vector form, can be written

$$\frac{d\bar{w}}{d\hat{T}_e} = \bar{F}(\bar{w}, \hat{T}_e) , \tag{6.7}$$

where $\bar{w} = \bar{w}(\hat{u}, \hat{T}_h, \hat{z})$. Then

$$\bar{w}_{n+1} = \bar{w}_n + \Delta \left\{ [I] - \frac{\Delta}{2}[A_n] \right\}^{-1} \left[\bar{F}_n + \frac{\Delta}{2} \left(\frac{\partial \bar{F}}{\partial \hat{T}_e} \right)_n \right] \tag{6.8}$$

where Δ is the step size, $[I]$ the identity matrix, and $[A_{ij}]_n = \left(\dfrac{\partial \bar{F}_i}{\partial \bar{w}_j} \right)_n$, $i,j=1,2,3$. Matrix $[A]$ is evaluated numerically at each step.

To obtain the spatial distribution of the variables, numerical integration of (6.2) is required. Once the spatial distribution is known, the induced electric field and charge separation can be computed.[5]

The computations, which were performed on the Brown University IBM 360 model 67 computer, require less than 5 minutes to perform.

VII. RESULTS AND DISCUSSION

Numerical examples have been calculated for microscopic models of argon and helium. The data are chosen from Ref. 5 (Figs. 1,2) and Ref. 11 (Figs. 3-10). All the results obtained for the collisional relaxation layer and the transport shock are plotted as functions of the physical distance $\underline{x}$.

Both the inner solution ($\underline{a}$ to $\underline{b}$) and the complete solution ($\underline{a}$ to $\underline{c}$) discussed here are true shock waves in the sense of nonlinear sound waves. Although the interaction between electrons and heavy particles is weak, the electrons are constrained by electrical forces and are forced to shock. The transport shock and the collisional layer are interrelated, since the former arises as the inner solution to the latter. Since the flow over the inner solution is not totally frozen with respect to population of the excited and ionized levels, ionization and excitation rates must be included over the inner solution. Inelastic collisions are responsible for cooling the electrons as the flow approaches the collisional layer, and they thus prevent the light and heavy species from reaching thermal equilibrium on the small scale of the transport shock, as would otherwise occur through the elastic collision mechanism.[5] The inclusion of the inelastic collisions is also responsible for the new Rankine-Hugoniot state relation replacing $\left[T_e\right]_b^a = 0$ across the transport shock. Although Foley and Clarke did not obtain the correct value of T_e behind an unstructured transport shock, the electron temperature catches up to its correct value very quickly at the beginning of the collisional layer for their numerical examples. In the context of their assumptions, their treatment of T_e across the transport shock is self consistent. However, an incorrect initial value in T_e for

the structure of the collisional layer could give substantial discrepancies in other dependent variables (cf. Fig. 3).

Our results for the outer solution were anticipated, on numerical grounds, in Refs. 4 and 15, although our treatment of β over the collisional layer is different from Ref. 4. In our model, no assumption is made that every excited atom created will be immediately ionized and thus a more realistic treatment of the ionization process is provided. Figs. 1 and 3 show typical solutions over the collisional layer for the conditions noted. The asymptotic result is compared to the exact solution obtained by solving simultaneously Eqs. (3.20) - (3.26) neglecting the transport properties.

As the transport phenomena are included in structuring the inner solution, an electron precursor evidently appears due to the electron thermal conductivity (cf. Figs. 2, 4-10). The sharp rise in electron temperature that might be expected behind the transport shock as a consequence of the jump condition $\left[T_e \right]_b^a = 0$, actually occurs at its beginning due to K_e .

Over the inner solution, the actual rise in the degree of ionization, for all the examples evaluated, is less than 6%. In Fig. 2, the inner solution was computed twice for two disparate values of β . We can see that the two results are almost identical. This is due to the fact that β is everywhere much smaller than α , its numerical value not affecting the results. Thus, our results clearly validate the treatment of α and β as constant at their initial values over the transport shock.

If we are not interested in the transport effects, it is possible to disregard the structure of the inner solution. However, with the use of our jump conditions, we can evaluate the correct flow variables behind the

transport shock. One could neglect the structure of the heavy particle transport properties (cf. Figs. 5, 8, 10) and treat this as a discontinuity representing an "innermost" solution within our inner solution, structured solely by electron conductivity; but this simplification will not always be possible, because matching difficulties will appear. This innermost solution can not be realistically embedded by an asymptotic argument on the length scale of the inner solution. For the numerical examples evaluated, the thickness of this innermost solution is about 25-30% of the total thickness of the inner solutions given.

There are some cases in which the asymptotic method discussed here will not give satisfactory results particularly in the case of the lighter gases, depending on how strongly the gas parameters will tend to their respective limits (4.1) and (4.2). If the gas is lighter (δ diminishes), the elastic coupling between electrons and heavy particles increases. For helium, for instance, only one of the numerical examples considered (cf. Fig. 6) was successful, the one corresponding to the smaller degree of ionization of the upstream flow ($\alpha_a = 0.0412$). As α_a increases ($\alpha_a \sim 0.1$), the electron temperature behind the transport shock increases, due to coupling effect, by a factor of 2 with respect to a similar argon example. At these high temperatures, and with the initial concentration of electrons corresponding to $\alpha_a = 0.1$, λ_e and λ_α can become comparable and our asymptotic procedure will fail, since appreciable ionization will occur inside the transport shock. The inner solution for the helium case we have been able to evaluate is shown in Fig. 6. The outer solution for this example can be found in Ref. 15.

All the assumptions upon which this model is based are completely justified _a posteriori_. The values obtained for the induced electric field

and charge separation are indeed very small. The initially frozen elastic
and inelastic collision assumption used to structure the shock is also
justified; a difference of 2 - 3% in the results appears according as it
is used (as shown explicitly in Eq. (6.5)) or not used.

Finally, we must mention the work by Magretova, Pashchenko and Razier[19]
who studied a strong shock in air. Taking into account the thermal con-
ductivity of the electrons as the only transport mechanism, they found an
electron precursor. The heating of the electron gas is said to produce
appreciable ionization before the heavy gas is shocked. With our model,
no such ionization appears in the electron precursor for any of the exam-
ples we have evaluated.

The method presented herein can be used, if desired, together with
the work of Foley and Clarke[11] to obtain the full structure of a shock
wave when radiative as well as collisional effects are to be taken into
account, providing a rational description of the kinetics of the collisional
and radiative ionization reactions at high temperatures.

APPENDIX: ALTERNATE ARGUMENT

Over the outer solution it is clear that $\frac{1}{\alpha}\frac{d\beta}{d\eta}$ is much smaller than $\frac{1}{\alpha}\frac{d\alpha}{d\eta}$ as seen from (3.25) and (3.26) under the asymptotic argument in Section IV. Therefore, in (3.24) we can neglect the former term as compared to the latter. If in (3.24) we substitute $\frac{1}{\alpha}\frac{d\alpha}{d\eta}$ by its corresponding expression $\hat{I}_1$ and neglect the left hand side which is $0\left(\frac{1}{\hat{T}_j}\right)$, and $\frac{1}{\alpha}\frac{d\beta}{d\eta}$

we get

$$\Gamma_1 \frac{\hat{T}_e^{1/2}}{\hat{u}}\left(\hat{T}_h - \hat{T}_e\right) - \left[1 - \frac{\alpha^2}{1-\alpha-\beta}\frac{1-\alpha_E-\beta_E}{\alpha_E^2}\right] - \Gamma_2\left[1 - \frac{\alpha^2}{\beta}\frac{\beta_E}{\alpha_E^2}\right] = 0 . \qquad (Ap.1)$$

Now, from (3.26), we can write

$$\Gamma_2\left[1 - \frac{\alpha^2}{\beta}\frac{\beta_E}{\alpha_E^2}\right] = \frac{\kappa_{1-2}}{\kappa_{1-c}}\left[1 - \frac{\beta}{1-\alpha-\beta}\frac{1-\alpha_E-\beta_E}{\beta_E}\right] + 0\left(\frac{\beta}{\alpha}\right) . \qquad (Ap.2)$$

Thus (Ap.1) can alternately be written as

$$\Gamma_1 \frac{\hat{T}_e^{1/2}}{\hat{u}}\left(\hat{T}_h - \hat{T}_e\right) - \left[1 - \frac{\alpha^2}{1-\alpha-\beta}\frac{1-\alpha_E-\beta_E}{\alpha_E^2}\right] - \frac{\kappa_{1-2}}{\kappa_{1-c}}\left[1 - \frac{\beta}{1-\alpha-\beta}\frac{1-\alpha_E-\beta_E}{\beta_E}\right] = 0 . (Ap.3)$$

We can verify very easily that (Ap.3) is precisely the form (3.24) takes on (besides a factor of

$$\frac{\hat{T}_\ell}{\hat{T}_j} = 1 - 0\left(\frac{1}{\hat{T}_j}\right)$$

multiplying the last term) when we substitute in it $\frac{1}{\alpha}\frac{d\alpha}{d\eta}$ and $\frac{1}{\alpha}\frac{d\beta}{d\eta}$ by

their corresponding expressions $\hat{I}_1$ and $\hat{I}_2$. The difference between (Ap.1) and (Ap.3) is seen to be of a higher order.

On physical grounds, we prefer Eq. (Ap.3) to Eq. (Ap.1), because (Ap.3) states explicitly that, over the outer solution, the three difficult processes introduced in Section II, namely energy transfer between heavy and light species through elastic collisions, ionization from the ground level, and excitation from the ground level give the energy balance of the electrons.

The above argument also holds in the discussion of the inner solution since $\frac{1}{\alpha}\frac{d\beta}{d\zeta}$ can be neglected as compared to $\frac{1}{\alpha}\frac{d\alpha}{d\zeta}$, because β is everywhere much smaller than α according to the microscopic model of Section II. We also prefer, for the reasons explained above, to substitute in (4.13) $\frac{d\alpha}{d\zeta}$ and $\frac{d\beta}{d\zeta}$ by their expressions in the right of (4.14) and (4.15) respectively, to get

$$\frac{3}{2}\frac{d\hat{T}_e}{d\zeta} + \frac{\hat{T}_e}{\hat{u}}\frac{d\hat{u}}{d\zeta} - \frac{1}{\alpha}\frac{d}{d\zeta}\left[\frac{\lambda_{Ke}}{\lambda_e}\alpha\rho\hat{T}_e^{1/2}\frac{d\hat{T}_e}{d\zeta}\right] =$$

$$\frac{\hat{T}_e^{1/2}}{\hat{u}}\left(\hat{T}_h - \hat{T}_e\right) - \frac{1}{\Gamma_1}\left\{\left[1 - \frac{\alpha^2}{1-\alpha-\beta}\frac{1-\alpha_E-\beta_E}{\alpha_E^2}\right] + \frac{\hat{T}_\ell}{\hat{T}_j}\frac{\kappa_{1-2}}{\kappa_{1-c}}\left[1 - \frac{\beta}{1-\alpha-\beta}\frac{1-\alpha_E-\beta_E}{\beta_E}\right]\right\}$$

$$- \frac{\Gamma_2}{\Gamma_1}\left(1 - \frac{\hat{T}_\ell}{\hat{T}_j}\right)\left[1 - \frac{\alpha^2}{\beta}\frac{\beta_E}{\alpha_E^2}\right] \quad . \tag{Ap.4}$$

It is clear that the last term in the right of (Ap.4) can be neglected under (4.1c).

Thus we see that in the outer solution as well as in the inner solution, substituting the ionization and excitation rates by their corresponding expressions is equivalent to neglect the excitation rate as compared to the ionization rate, the difference between these two alternatives being higher order. However, we prefer the former to the latter because of its physical meaning, particularly over the collisional layer.

APPENDIX A

TRANSPORT PROPERTIES

The mathematical expressions for the different coefficients of viscosity and thermal conductivity are taken from Ref. 5. If σ_{ij} denotes the elastic collision cross section for an encounter between particles of the ith and jth species and subscripts $\underline{a}$, $\underline{e}$, and $\underline{i}$ refer to atoms (in the ground and excited levels), electrons and ions respectively, we have

Heavy transport coefficients

The coefficient of shear viscosity of the mixture is

$$\mu_h = \rho(RT_h)^{1/2}\lambda_\mu \, , \tag{A.1}$$

where λ_μ is a characteristic length defining the viscosity of the heavy particles. We can express λ_μ in terms of the different elastic cross sections and therefore in terms of the dependent variables, i.e.

$$\lambda_\mu \equiv \frac{5\sqrt{\pi}}{6} \frac{1}{n_a\sigma_{aa}} \left[\frac{1-\alpha}{1 + \dfrac{n_e\sigma_{ia}}{n_a\sigma_{aa}}} + \frac{\sigma_{aa}}{\sigma_{ia}} \frac{\alpha}{1 + \dfrac{n_e\sigma_{ii}}{n_a\sigma_{ia}}} \right], \tag{A.2}$$

or

$$\lambda_\mu \equiv \frac{5\sqrt{\pi}}{6} \frac{m_h}{\rho} \frac{1}{(1-\alpha)\sigma_{aa}} \left[\frac{1-\alpha}{1 + \dfrac{\alpha}{1-\alpha}\dfrac{\sigma_{ia}}{\sigma_{aa}}} + \frac{\sigma_{aa}}{\sigma_{ia}} \frac{\alpha}{1 + \dfrac{\alpha}{1-\alpha}\dfrac{\sigma_{ii}}{\sigma_{ia}}} \right] \tag{A.3}$$

The coefficient of thermal conductivity of the heavy particles K_h , is given by

$$K_h = \rho R(RT_h)^{1/2} \lambda_{Kh} \, , \tag{A.4}$$

λ_{Kh} being a characteristic length for the heavy thermal conductivity and it is defined by

$$\lambda_{Kh} \equiv \frac{75\sqrt{\pi}}{64} \frac{m_h}{\rho} \frac{1}{(1-\alpha)\sigma_{aa}} \left[\frac{1-\alpha}{1 + \frac{\alpha}{1-\alpha} \frac{\sigma_{ia}}{\sigma_{aa}}} + \frac{\sigma_{aa}}{\sigma_{ia}} \frac{\alpha}{1 + \frac{\alpha}{1-\alpha} \frac{\sigma_{ii}}{\sigma_{ia}}} \right] \, . \tag{A.5}$$

From the definitions of λ_μ and λ_{Kh} , we can see that

$$\frac{\lambda_{Kh}}{\lambda_\mu} = \frac{75}{64} \frac{6}{5} = \frac{45}{32} \, . \tag{A.6}$$

Thus both lengths characterizing the transport properties of the heavy gas are almost the same.

Electron transport properties

The viscosity of the electrons can be neglected as compared to the viscosity of the heavies due to the small mass ratio of the two species. Since $\mu_e = 0$, the viscosity of the mixture will then be given by

$$\mu = \mu_h + \mu_e \equiv \mu_h \, . \tag{A.7}$$

The electron thermal conductivity is given by

$$K_e = \alpha R\rho(RT_e)^{1/2} \lambda_{Ke} \, , \tag{A.8}$$

where λ_{Ke} is a characteristic length for the electron thermal conductivity, defined by

$$\lambda_{Ke} \equiv \frac{75\sqrt{\pi}}{64} \frac{\delta}{n_e \sigma_{ei}} \left[(1+\sqrt{2})\left(1 + \frac{\sqrt{2}\, n_a \sigma_{ea}}{(1+\sqrt{2})n_e \sigma_{ei}}\right) \right]^{-1}$$

$$= \frac{75\sqrt{\pi}}{64} \frac{m_h}{\rho} \frac{\delta}{\alpha \sigma_{ei}} \left[(1+\sqrt{2})\left(1 + \frac{\sqrt{2}}{1+\sqrt{2}} \frac{1-\alpha}{\alpha} \frac{\sigma_{ea}}{\sigma_{ei}}\right) \right]^{-1} \tag{A.9}$$

The energy transfer between heavy and light species through elastic collisions E is given by[5]

$$E = (RT_e)^{1/2} \frac{T_h - T_e}{u} \frac{1}{\lambda_e} , \tag{A.10}$$

λ_e being a characteristic length defining this type of energy transfer, defined by

$$\lambda_e \equiv \frac{1}{8} \sqrt{\frac{\pi}{2}} \frac{m_h}{\rho} \frac{\delta}{\alpha \sigma_{ei}} \left[1 + \frac{1-\alpha}{\alpha} \frac{\sigma_{ea}}{\sigma_{ei}} \right]^{-1} \tag{A.11}$$

It is clear from (A.9) and (A.11) that both λ_{Ke} and λ_e are comparable lengths.

Moreover, on numerical grounds, and depending mainly on the flow conditions, the characteristic lengths defining the transport properties λ_μ, λ_{Kh}, and λ_{Ke} can be comparable, and therefore λ_μ/λ_{Ke}, $\lambda_{Kh}/\lambda_{Ke}$ can be non-neglibible quantities. Our results prove the validity of the above argument.

Since

$$\frac{\lambda_\mu}{\lambda_\alpha} = \frac{\lambda_\mu}{\lambda_{Ke}} \frac{\lambda_{Ke}}{\lambda_e} \frac{\lambda_e}{\lambda_\alpha} = 0\left(\frac{1}{T_j}\right) , \tag{A.12}$$

$$\frac{\lambda_{Kh}}{\lambda_\alpha} = \frac{\lambda_{Kh}}{\lambda_{Ke}} \frac{\lambda_{Ke}}{\lambda_e} \frac{\lambda_e}{\lambda_\alpha} = 0\left(\frac{1}{T_j}\right), \tag{A.13}$$

$$\frac{\lambda_{Ke}}{\lambda_\alpha} = \frac{\lambda_{Ke}}{\lambda_e} \frac{\lambda_e}{\lambda_\alpha} = 0\left(\frac{1}{T_j}\right), \tag{A.14}$$

We can neglect all the transport properties over the outer solution characterized by λ_α within the orders of magnitude and limits constructed in (4.1) and (4.2).

APPENDIX B

COLLISIONAL STATISTICS

In this appendix expressions for all the cross sections and reaction rates are provided for both argon and helium.

Elastic Cross Sections:

1. Argon: All the cross sections for argon are taken from Ref. 5. These cross sections in terms of the flow variables are:

$$\sigma_{ei} = \frac{\pi e^4}{2} \frac{\ell n \Lambda_e}{(kT_e)^2} \text{ cm}^2 \quad , \quad \Lambda_e = \frac{3}{2e^3} \left(\frac{k^3 T_e^3}{\pi n_e}\right)^{1/2} \tag{B.1}$$

$$\sigma_{ii} = \frac{\pi e^4}{2} \frac{\ell n \Lambda_i}{(kT_h)^2} \text{ cm}^2 \quad , \quad \Lambda_i = \frac{3}{2e^3} \left(\frac{k^3 T_h^3}{\pi n_e}\right)^{1/2} \tag{B.3}$$

where e is the magnitude of the electronic charge, and k the Boltzmann constant. The remaining cross sections are

$$\sigma_{aa} = \frac{1.7}{T_h^{1/4}} \times 10^{-14} \text{cm}^2 \quad , \tag{B.3}$$

$$\sigma_{ia} = 1.4 \times 10^{-14} \text{ cm}^2 \quad ,$$

$$\sigma_{ea} = \begin{cases} [-0.35 + (0.775 \times 10^{-4})T_e] \times 10^{-16} \text{cm}^2 & \text{for } T_e > 10^4 \text{ °K} \\ \\ [0.39 - (0.551 \times 10^{-4})T_e + (0.595 \times 10^{-8})T_e^2] \times 10^{-16} \text{cm}^2 & \text{for} \\ \\ \hspace{8cm} T_e \le 10^4 \text{ °K} \end{cases} \tag{B.4}$$

2. Helium: The cross sections for collisions between charged particles are the same as for argon, i.e., σ_{ei} and σ_{ii} are given by (B.1) and (B.2), since the cross sections are independent of the masses of the particles involved.

From Ref. 11

$$\sigma_{ea} = 5 \times 10^{-16} cm^2 \ . \tag{B.6}$$

From Hirchsfelder et al,[20] the average cross section for the computation of viscosity and thermal conductivity is given by

$$\overline{Q}^{(2.2)} = \frac{1}{4} \int_0^\infty x^3 Q^{(2)}(xkT)\exp(-x)dx \ , \tag{B.7}$$

where $Q^{(2)}$ denotes the interaction potential for the colliding molecules.

From Ref. 12, the interaction potential for an atom and an ion is given by the empirical expression:

$$Q^{(2)} = [48.0 - 6.96\ln(xkT+0.4) \times 10^{-16} cm^2 \tag{B.8}$$

expressing kT in eV . Expanding the logarithmic term

$$\ln(xkT+0.4) = \ln 0.4 + 2\left[\frac{xkT}{xkT+0.8} + \frac{1}{3}\left(\frac{xkT}{xkT+0.8}\right)^3 + ---\right]$$

$$\simeq \ln 0.4 + 2\frac{T}{\frac{10^4}{x} + T} \ .$$

Substituting (B.9) into (B.7), we obtain

$$\sigma_{ia} = \left\{\frac{1}{4}\Gamma(4)[48.0 - 6.96\ln 0.4] - 6.96 \times 2 \int_0^\infty \frac{Tx^3}{\frac{10^4}{x} + T}\exp(-x)dx\right\} \times 10^{-16} cm^2 \ . \tag{B.10}$$

Since $0 < \dfrac{T}{\dfrac{10^4}{x} + T} < 1$, we take an average for the above integral to get

$$\sigma_{ia} = 71 \times 10^{-16} \, cm^2 \, . \qquad (B.11)$$

From Monchick,[21] the average cross section for atom-atom collisions is given by

$$\sigma = \frac{8\alpha^2 \rho^2 I_{(2,2)}}{3!\left(1 - \frac{1}{3}\right)} = 2\alpha^2 \rho^2 I_{(2,2)} \, , \qquad (B.12)$$

where $\alpha = \ln \dfrac{A}{kT}$ and A and ρ are related in the expression for the interaction potential

$$\phi = A \exp(-r/\rho) \, , \qquad (B.13)$$

with ρ in angstroms. Monchick gives a tabulation for $I_{(2,2)}$ as function of α . From Ref. 22 we have for the H_e-H_e interaction

$$A = 157 \, ev, \qquad \rho = 1/3.93 \, \overset{o}{A} \, . \qquad (B.14)$$

For our range of temperature $300^\circ \leq T_h \leq 130000^\circ$, we can extrapolate Monchick's results. The difference in the values of $I_{(2,2)}$ is not very significant however. By taking an intermediate value

$$I_{(2,2)} = 0.512267 \, , \qquad (B.15)$$

corresponding to $\alpha = 4.5$, we obtain

$$\sigma_{aa} = 0.066291 \, [14.4137 - \ln T_h]^2 \times 10^{-16} \, cm^2 \, . \qquad (B.16)$$

Inelastic Processes

All the inelastic processes considered are those involving chemical reactions by electron impact as given by (2.1).

According to these reactions, we can write

$$\frac{dn_e}{dt} = \kappa_{1-c} n_1 n_e - \kappa_{c-1} n_e^3 + \kappa_{2-c} n_2 n_e - \kappa_{c-2} n_e^3 , \qquad (B.17)$$

$$\frac{dn_2}{dt} = \kappa_{1-2} n_1 n_e - \kappa_{2-1} n_2 n_e + \kappa_{c-2} n_e^3 - \kappa_{2-c} n_2 n_e , \qquad (B.18)$$

where in (B.17) and (B.18) the number densities can be written in terms of ρ , α and β . We know from equilibrium considerations that

$$\kappa_{2-1} = \kappa_{1-2} \left(\frac{n_1}{n_2}\right)_E = \kappa_{1-2} \frac{1-\alpha_E-\beta_E}{\beta_E} , \qquad (B.19)$$

$$\kappa_{c-1} = \kappa_{1-c} \left(\frac{n_1}{n_e^2}\right)_E = \kappa_{1-c} \frac{m_h}{\rho} \frac{1-\alpha_E-\beta_E}{\alpha_E^2} , \qquad (B.20)$$

$$\kappa_{c-2} = \kappa_{2-c} \left(\frac{n_2}{n_e^2}\right)_E = \kappa_{2-c} \frac{m_h}{\rho} \frac{\beta_E}{\alpha_E^2} , \qquad (B.21)$$

where E denotes equilibrium conditions.

We write α_E and β_E in terms of the dependent variables. Then

$$\frac{1-\alpha_E-\beta_E}{\alpha_E^2} = \frac{1}{2} \frac{\rho}{m_h} \frac{g_0 + g_1 \exp(-T_\ell/T_e)}{g_0^+ + g_1^+ \exp(-T_p/T_e)} \frac{\exp(T_j/T_e)}{\left[\frac{2\pi m_e kT_e}{h^2}\right]^{3/2}} , \qquad (B.22)$$

$$\frac{\beta_E}{\alpha_E^2} = \frac{1}{2} \frac{\rho}{m_h} \frac{g_1}{g_0^+ + g_1^+ \exp(-T_p/T_e)} \frac{\exp[(T_j-T_\ell)/T_e]}{\left[\dfrac{2\pi m_e kT_e}{h^2}\right]^{3/2}} \quad , \tag{B.23}$$

$$\frac{1-\alpha_E-\beta_E}{\beta_E} = 1 + \frac{g_0}{g_1} \exp(T_\ell/T_e) \quad , \tag{B.24}$$

where   k   is the Boltzmann constant,   h   the Planck constant, and g_i and

g_i^+ are the degeneracy factors in the electronic partition functions for

atoms and ions respectively.

We now need expressions for the forward reaction rate coefficients.

From Refs. 16 and 17 we have

$$\kappa_{p-q} = \frac{(3.84\times10^{-6})y^t \exp(-y)}{A^{1/4}\left(y^2 + \frac{7}{4}y + \frac{1}{g}\right)} \cdot \chi_{p-q}^{-1.5} \ \text{cm}^3/\text{s} \tag{B.25}$$

where χ_{p-q} is the potential difference between levels   p   and   q

expressed in   eV , and

$$A = \frac{\chi_{p-c}}{\chi_{p-q}} \ , \qquad y = \frac{\chi_{p-q}}{kT_e} \ , \qquad t = \frac{A+30}{10A+25} \quad . \tag{B.26}$$

The numerical values taken for argon and helium are

$$\text{Helium} \ \left\{ \begin{array}{l} g_0 = 1 \ , \quad g_1 = 16 \ , \quad g_0^+ = 2 \ , \quad g_1^+ = 0 \ , \tag{B.27} \\[2ex] T_j = 285000^\circ K \ , \quad T_\ell = 244800^\circ K \ , \tag{B.28} \end{array} \right.$$

and

$$\text{Argon} \begin{cases} g_0 = 1 , & g_1 = 12 , & g_0^+ = 4 , & g_1^+ = 2 , & \text{(B.29)} \\ T_j = 183000^\circ K , & T_j = 134020^\circ K , & T_p = 2065^\circ K . & & \text{(B.30)} \end{cases}$$

Expressions (B.22) - (B.24) are to be substituted in the rate equations for the population of the excited and ionized levels in the appropriate dimensionless form defined in Section III.

ACKNOWLEDGMENTS

LIST OF CAPTIONS

FIG. 1. Outer solution, Argon. $p_a = 1.5 \times 10^{-4}$ atm., $\left(T_h\right)_a = \left(T_e\right)_a = 1000°K$, $T_c = 11700°K$, $\alpha_a = 0.1 \neq \left(\alpha_E\right)_a$, $\beta_a = 0.0001 \neq \left(\beta_E\right)_a$. Solid lines: Asymptotic solution. Broken lines: Exact solution for same initial conditions. $\bar{T}_i = T_i/\left(T_h\right)_b$.

FIG. 2. Inner solution, Argon. $p_a = 1.5 \times 10^{-4}$ atm., $\left(T_h\right)_a = \left(T_e\right)_a = 1000°K$. $T_c = 11700°K$, $\alpha_a = 0.1 \neq \left(\alpha_E\right)_a$. Solid lines. Asymptotic results for $\beta_a = 0.0001 \neq \left(\beta_E\right)_a$. Dotted lines: Asymptotic results for $\beta_a = 0.00059 \neq \left(\beta_E\right)_a$. Broken lines: Ref. 5 results for same initial conditions but with no excited level in atom model. $\bar{u} = u/u_b$, $\bar{T}_i = T_i/\left(T_h\right)_b$.

FIG. 3. Outer solution, Argon. $p_a = 10^{-4}$ atm., $\left(T_h\right)_a = 961°K$, $\left(T_e\right)_a = 5451°K$, $T_c = 19460°K$, $\alpha_a = 0.231 \neq \left(\alpha_E\right)_a$, $\beta_a = 0.000219 \neq \left(\beta_E\right)_a$. Solid lines: Asymptotic solution. Dotted lines: Asymptotic solution for different initial conditions (Ref. 11). Broken lines: Exact solution for different initial conditions (Ref. 11).

FIG. 4. Inner solution, Argon. $p_a = 10^{-4}$ atm., $\left(T_h\right)_a = 961°K$, $\left(T_e\right)_a = 5451°K$, $T_c = 19460°K$, $\alpha_a = 0.231 \neq \left(\alpha_E\right)_a$, $\beta_a = 0.000219 \neq \left(\beta_E\right)_a$. Solid lines: Asymptotic solution. Broken lines: Ref. 11 results for different atom model. $\bar{\rho} = \rho/\rho_b$, $\bar{T}_i = T_i/\left(T_h\right)_b$.

FIG. 5. Inner solution, Argon. Same initial conditions as in Fig. 4 but without heavy particle transport properties. $\bar{\rho} = \rho/\rho_b$, $\bar{T}_i = T_i/\left(T_h\right)_b$.

FIG. 6. Inner solution, Helium. $p_a = 10^{-4}$ atm., $\left(T_h\right)_a = 600°K$, $\left(T_e\right)_a = 4500°K$, $T_c = 23400°K$, $\alpha_a = 0.0412 \neq \left(\alpha_E\right)_a$, $\beta_a = 0.0000539 \neq \left(\beta_E\right)_a$. $\bar{\rho} = \rho/\rho_b$, $\bar{T}_i = T_i/\left(T_h\right)_b$.

FIG. 7. Inner solution, Argon. $p_a = 10^{-3}$ atm., $\left(T_h\right)_a = 900°K$, $\left(T_e\right)_a = 6800°K$, $T_c = 22000°K$, $\alpha_a = 0.205 \neq \left(\alpha_E\right)_a$, $\beta_a = 0.000108 \neq \left(\beta_E\right)_a$. Solid lines: Asymptotic solution. Broken lines: Ref. 11 results for different atom model. $\bar{\rho} = \rho/\rho_b$, $\bar{T}_i = T_i/\left(T_h\right)_b$.

FIG. 8. Inner solution, Argon. Same initial conditions as in Fig. 7 but without heavy particle transport properties. $\bar{\rho} = \rho/\rho_b$, $\bar{T}_i = T_i/\left(T_h\right)_b$.

FIG. 9. Inner solution. Argon $p_a = 10^{-5}$ atm., $\left(T_h\right)_a = 970°K$, $\left(T_e\right)_a = 4600°K$, $T_c = 17000°K$, $\alpha_a = 0.250 \neq \left(\alpha_E\right)_a$, $\beta_a = 0.000482 \neq \left(\beta_E\right)_a$. Solid lines: Asymptotic solution. Broken lines: Ref. 11 results for different atom model $\bar{\rho} = \rho/\rho_b$, $\bar{T}_i = T_i/\left(T_h\right)_b$.

FIG. 10. Inner solution, Argon. Same initial conditions as in Fig. 9 but without heavy particle transport properties. $\bar{\rho} = \rho/\rho_b$, $\bar{T}_i = T_i/\left(T_h\right)_b$.
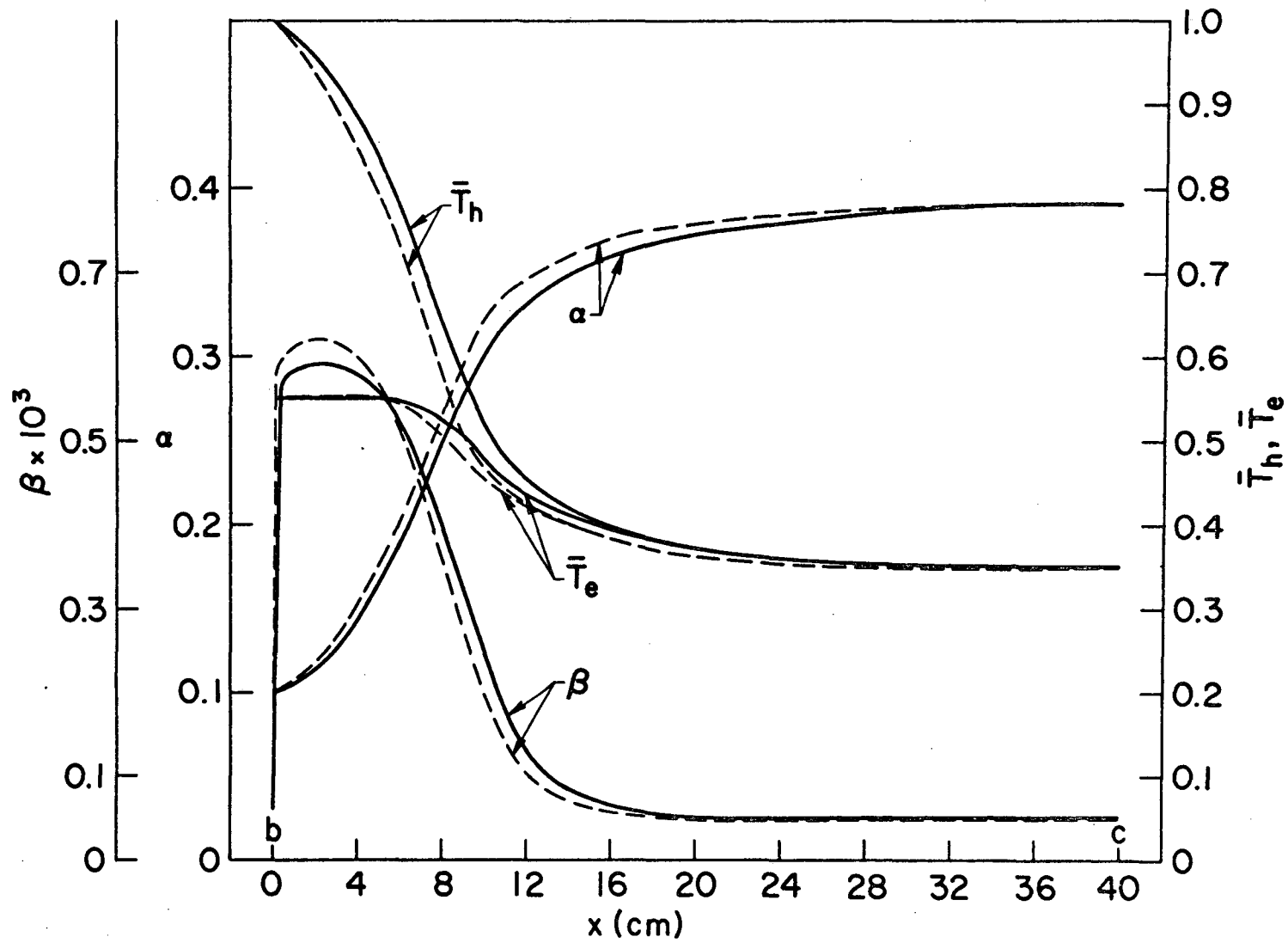
FIGURE I
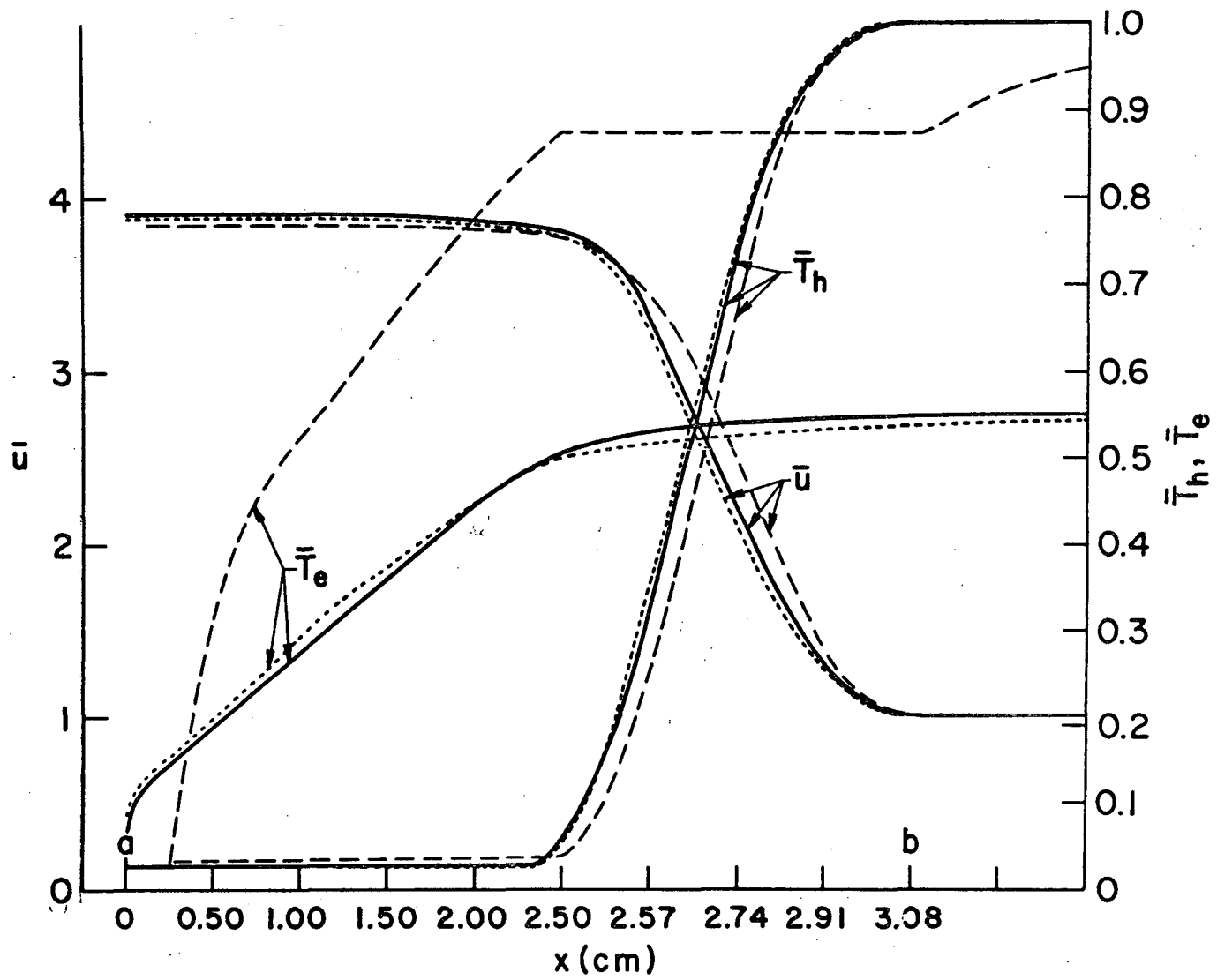
FIGURE 2
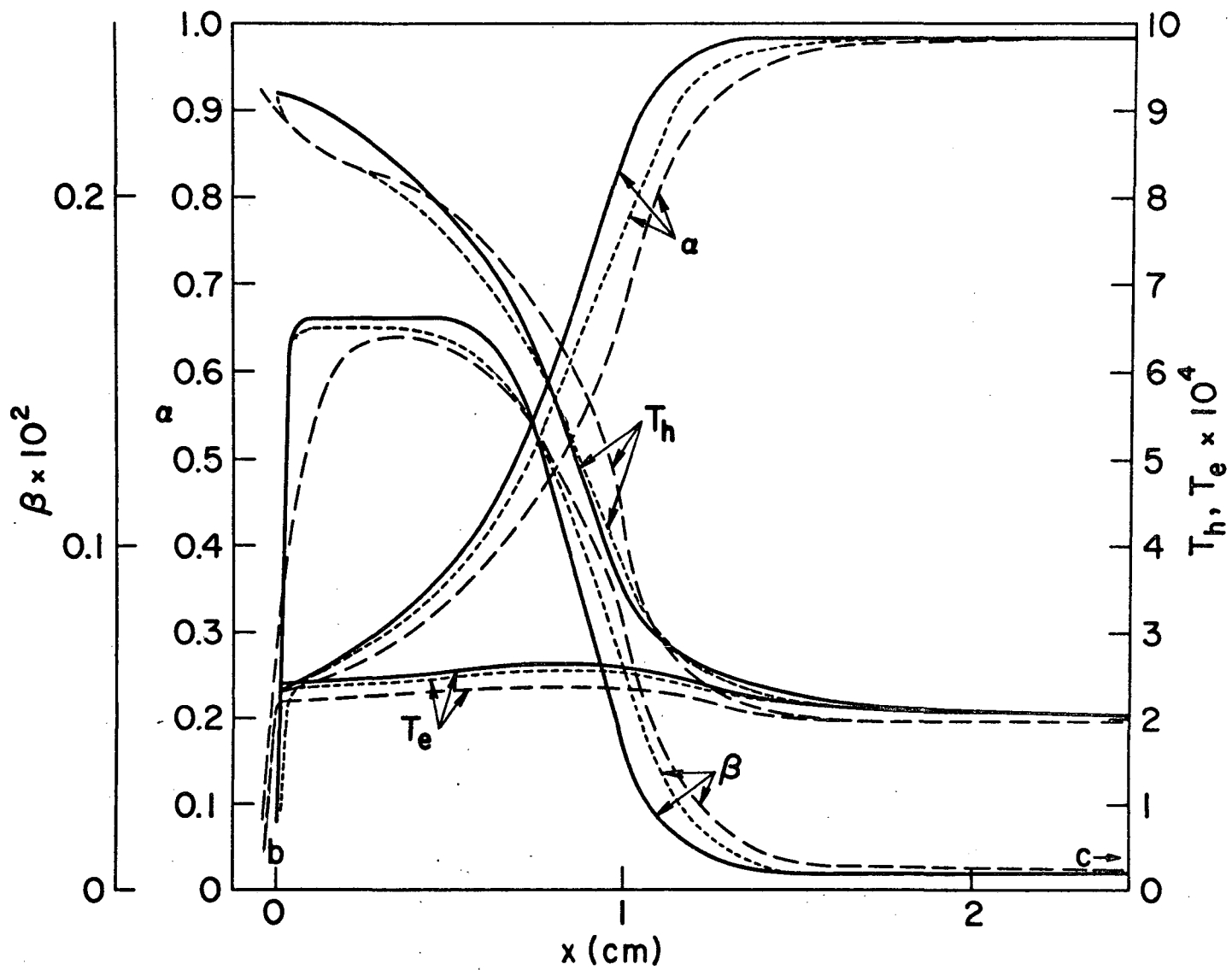
FIGURE 3
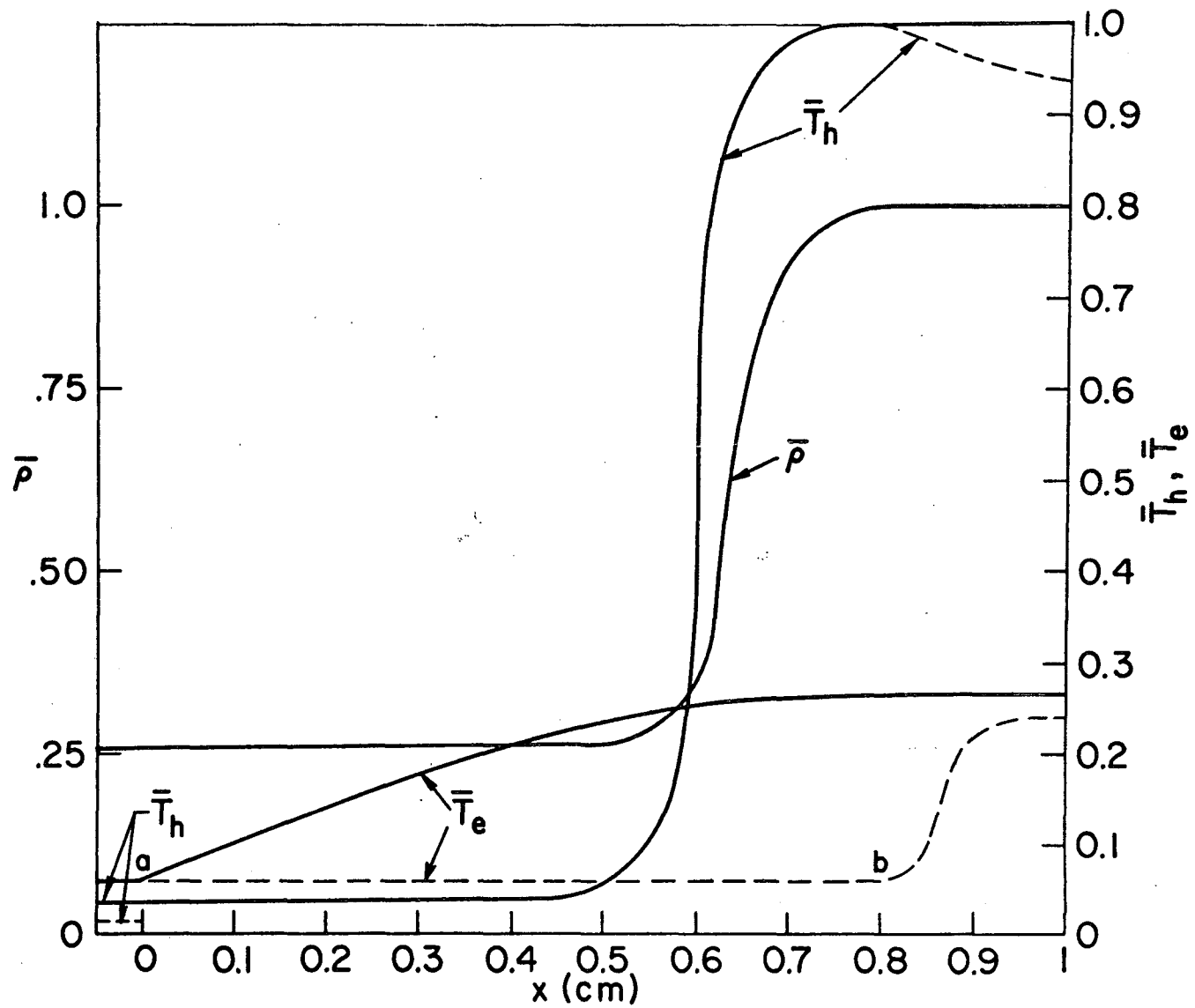
FIGURE 4
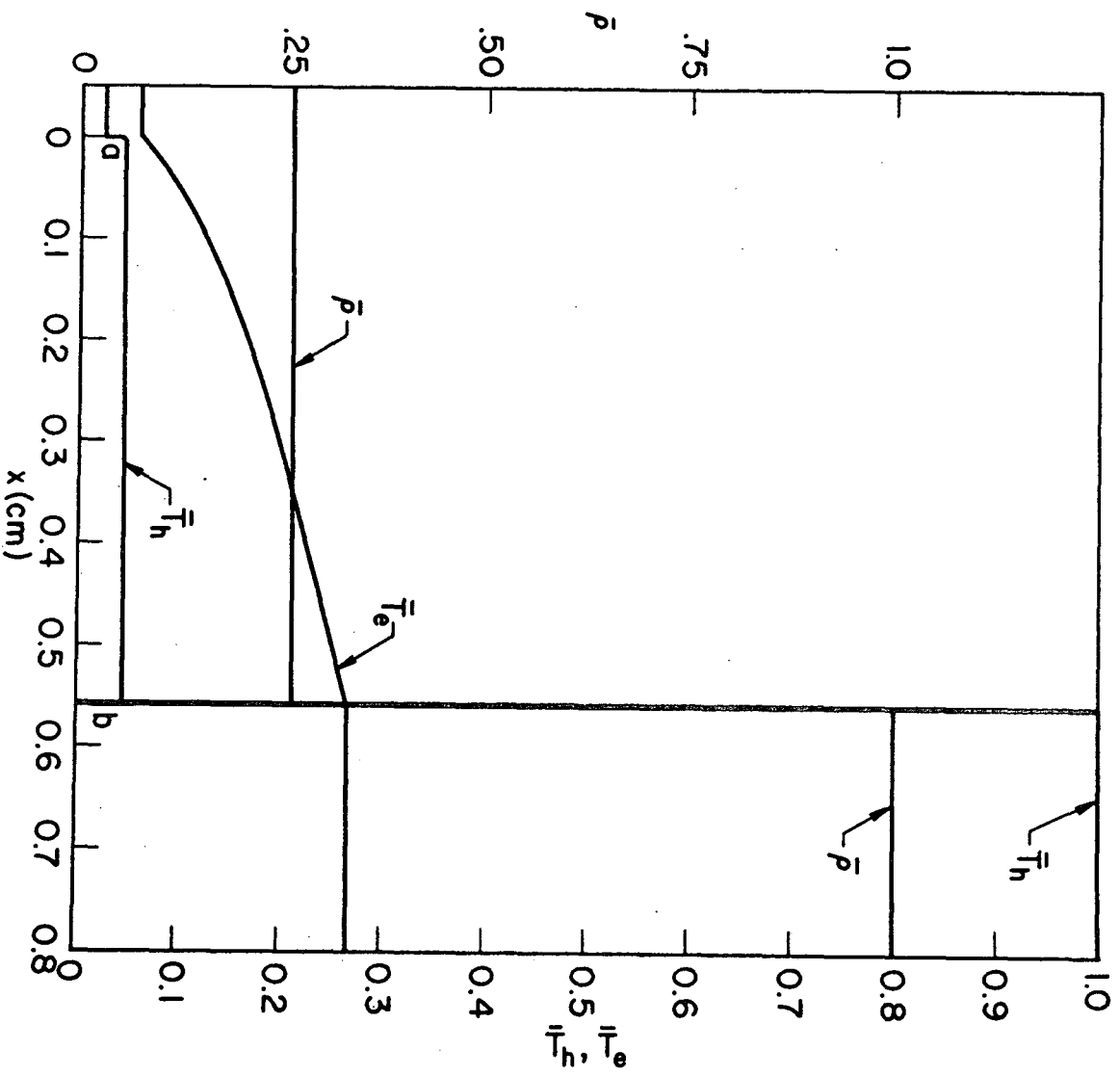
FIGURE 5
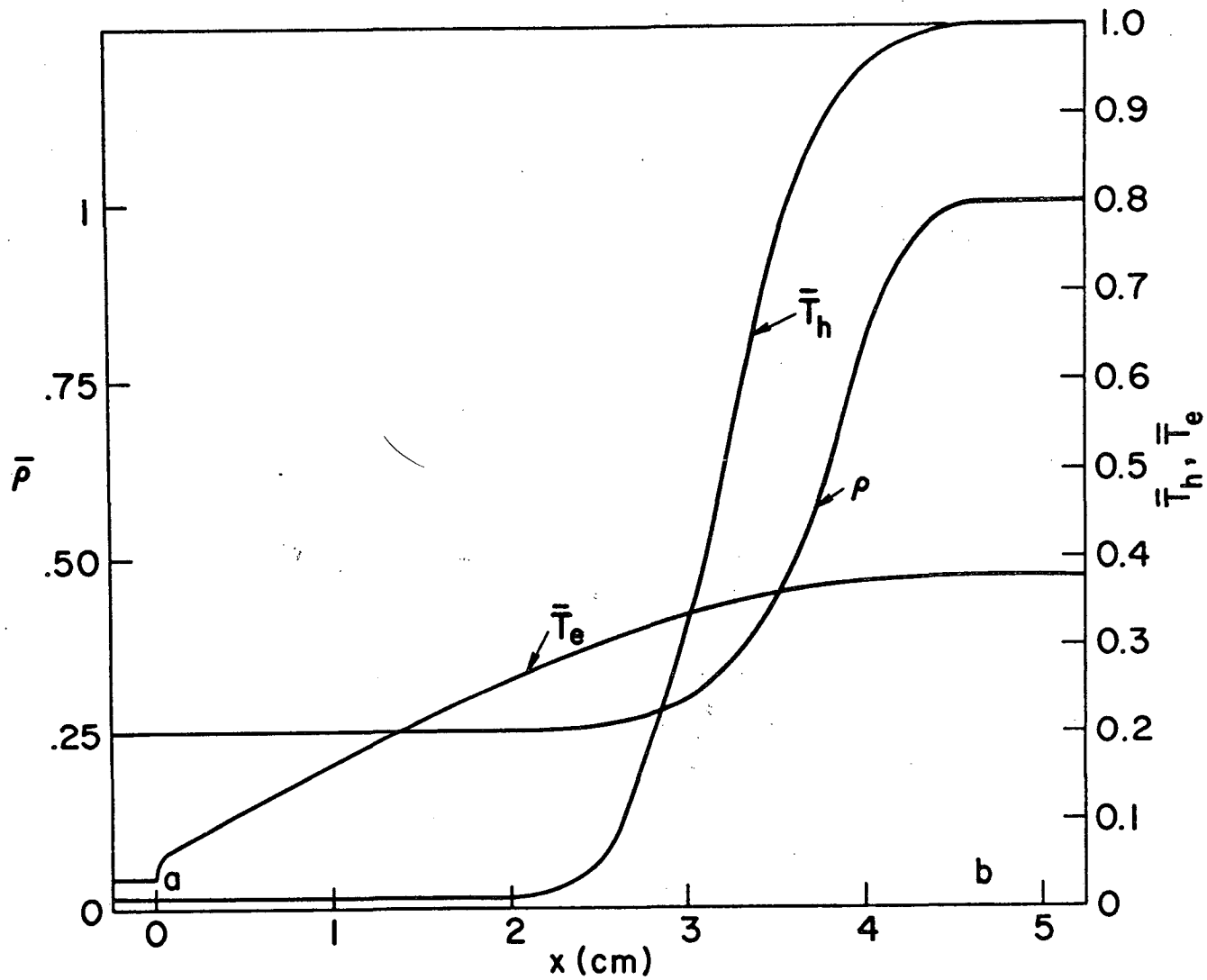
FIGURE 6
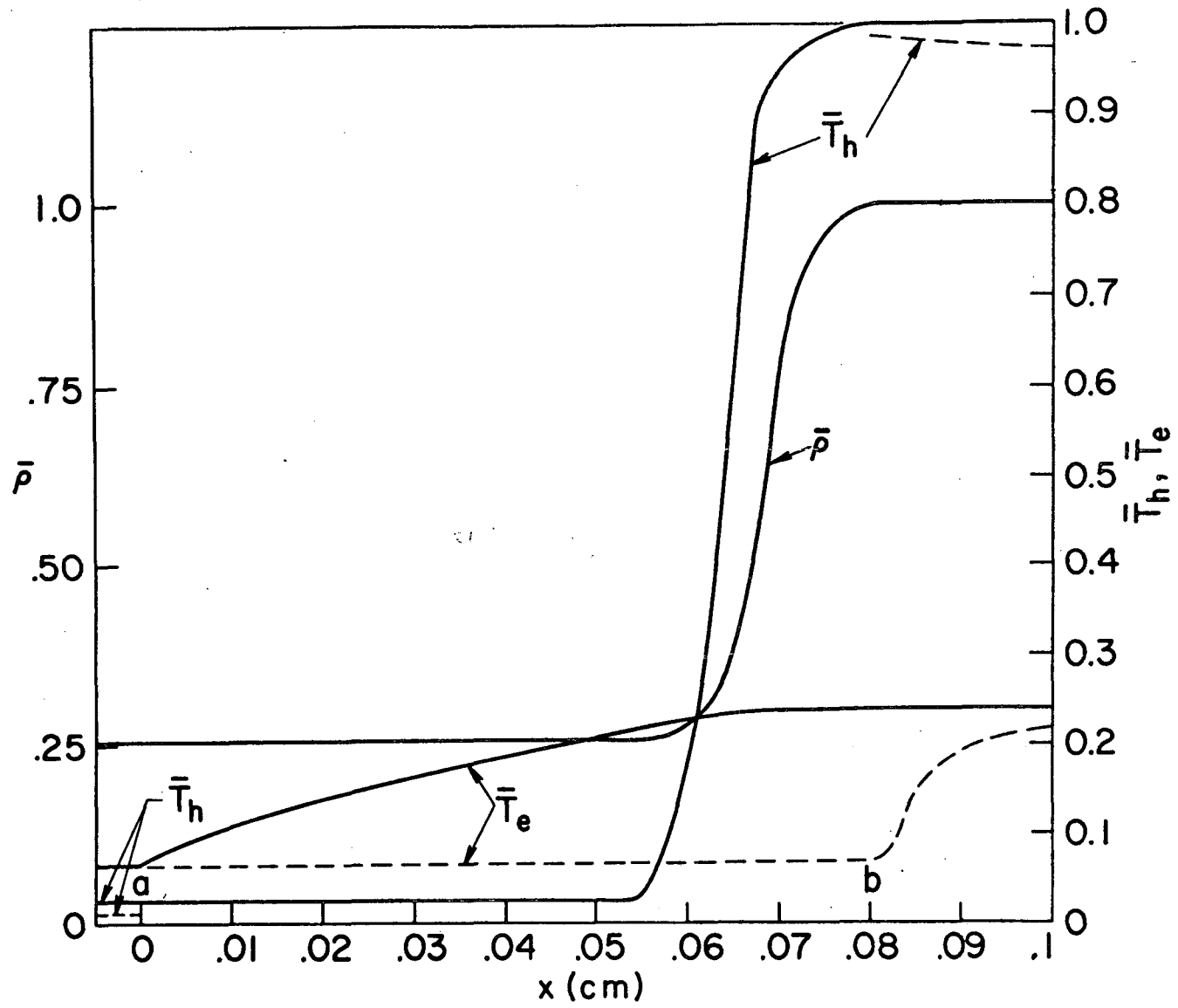
FIGURE 7
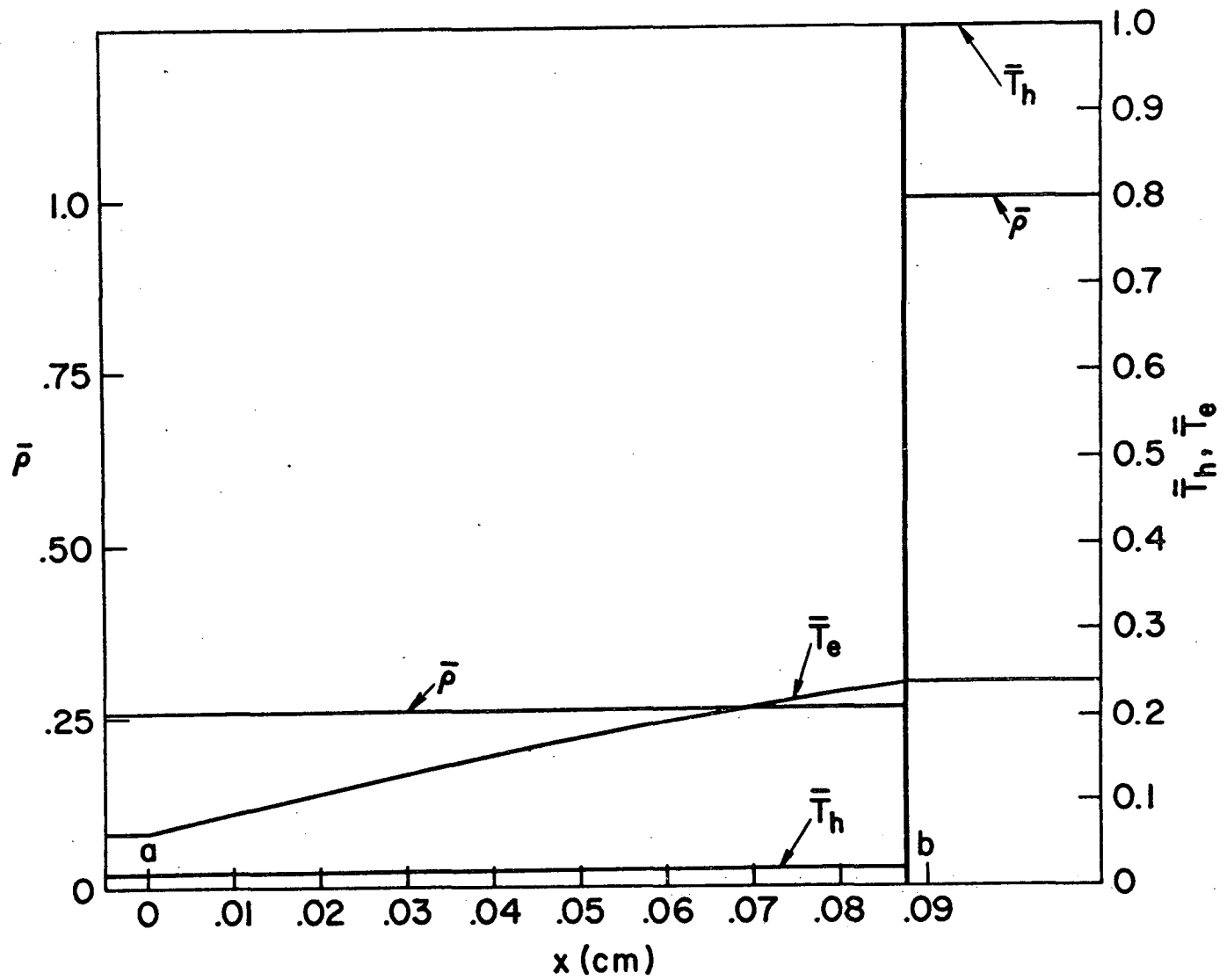
FIGURE 8
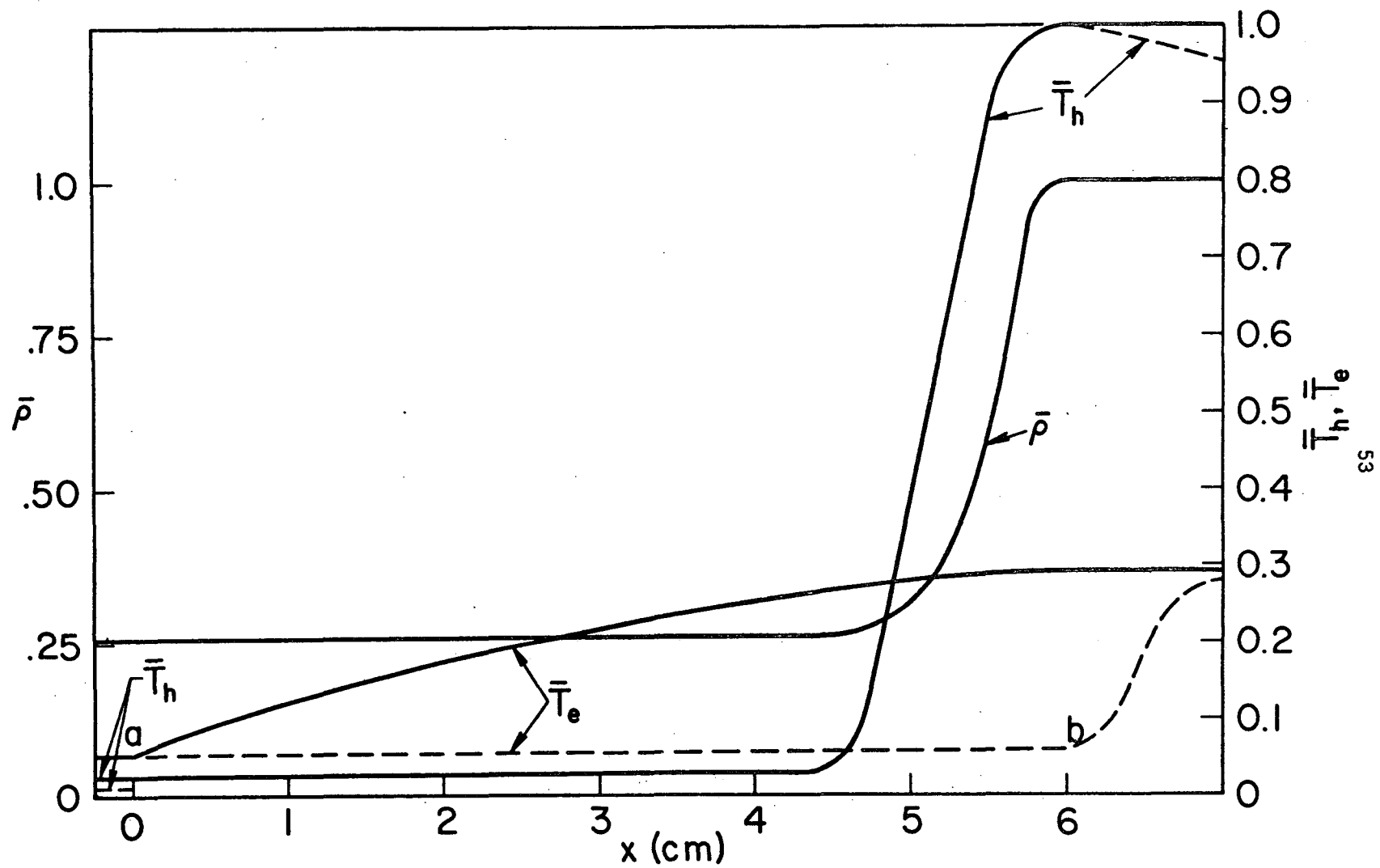
FIGURE 9
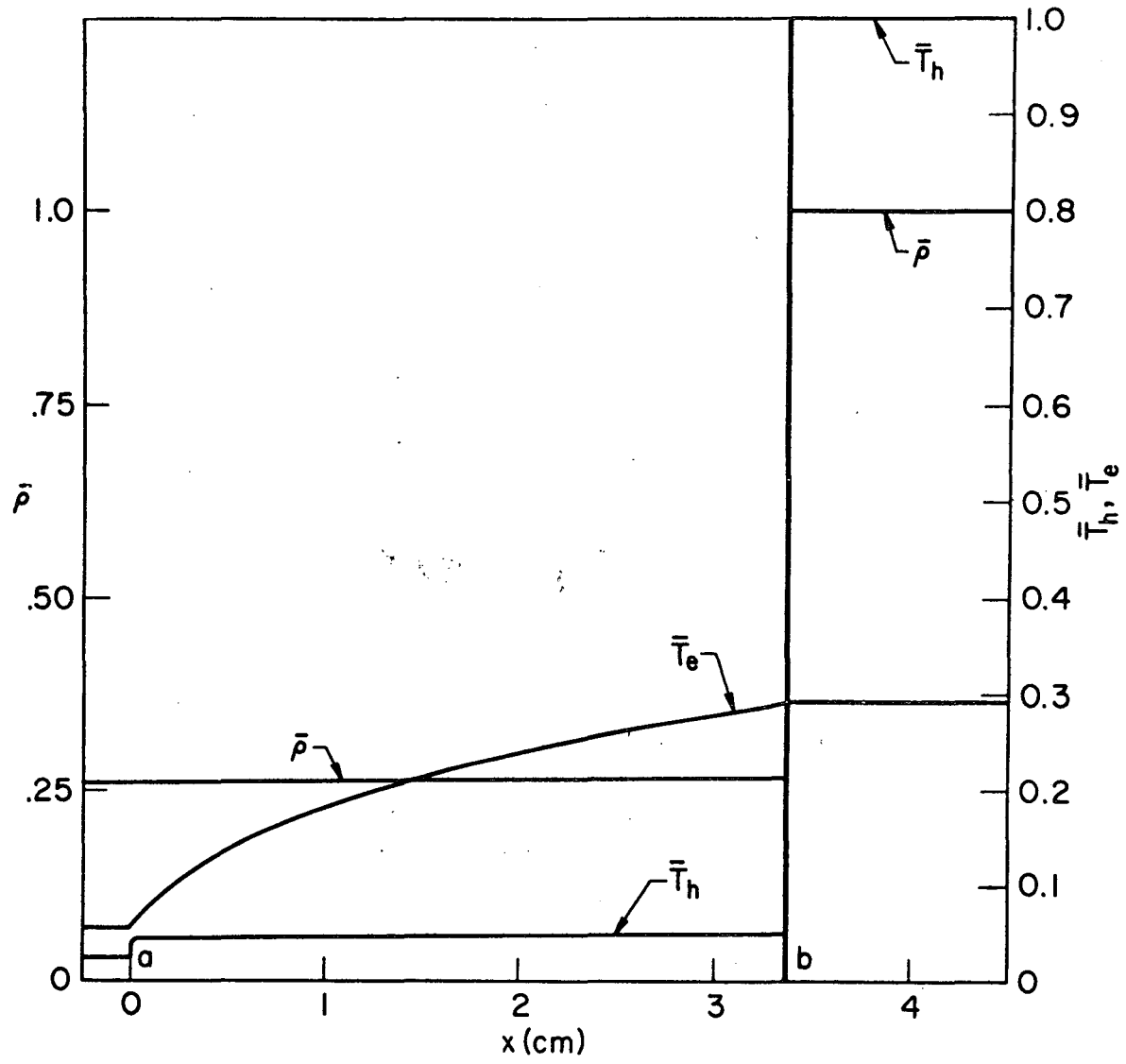
FIGURE 10

REFERENCES

1. H. Petschek and S. Byron, Ann. Phys. $\underline{1}$, 270 (1957).

2. M. I. Hoffert and H. Lien, Phys. Fluids $\underline{10}$. 1769 (1967).

3. H. F. Nelson, Univ. Missouri Rolla Report (1972).

4. L. M. Biberman, A. Kh. Mnatsakanyan and I. T. Yakubov, Sov. Phys. Uspheki $\underline{13}$, (1971).

5. M. Y. Jaffrin, Phys. Fluids $\underline{8}$, 606 (1965).

6. D. L. Chubb, Phys. Fluids $\underline{11}$, 2363 (1968).

7. J. H. Clarke and C. Ferrari, Phys. Fluids $\underline{8}$, 2121 (1965).

8. J. H. Clarke and M. Onorato, J. Appl. Mech. $\underline{37}$, 783 (1970).

9. A. N. Pirri and J. H. Clarke, AIAA J. $\underline{8}$, 1574 (1970).

10. A. V. Farnsworth and J. H. Clarke, Phys. Fluids $\underline{14}$, 1352 (1971).

11. W. Foley and J. H. Clarke, Accepted for Phys. Fluids, March 1972.

12. J. Lick and H. W. Emmons, Transport Properties of H_e from 200°K to 50000°K, Harvard University Press, Cambridge, Mass. (1965).

13. D. O. Hirchsfelder, Univ. of Wisconsin, C-M 880 (1956).

14. Ya B. Zeldovich and Yu. P. Raizer, Physics of Shock Waves and High Temperature Hydrodynamic Phenomena, Academic Press (1967).

15. J. H. Clarke and W. Foley, "XII Congress of the International Astronautical Federation," Sep. 1971, Brussels.

16. M. Gryzinski, Phys. Rev. $\underline{138}$, A336 (1965).

17. R. Goldstein, Jet. Propulsion Lab. Tech. Report 32-1372, Pasadena (1969).

18. H. Lomax and H. E. Bailey, NASA-TN-D-4109 (1967).

19. N. N. Magretova, M. G. Pashchenko and Yu. P. Raizer, PMTF $\underline{5}$, 11 (1970).

20. D. O. Hirchsfelder, Molecular Theory of Liquids and Gases, John Wiley and Son (1964).

21. L. Mondrick, Phys. Fluids $\underline{2}$, 695 (1958).

22. S. O. Colgate, J. E. Jordan, I. Admur and E. A. Mason, J. Chem.
     Phys. $\underline{J1}$, 968 (1969).